DEVELOPMENTAL DYNAMICS 246:7–27, 2017
DOI: 10.1002/DVDY.24466

RESEARCH ARTICLE

Concomitant Differentiation of a Population of Mouse Embryonic Stem Cells into Neuron-like Cells and Schwann cell–like Cells in a Slow-flow Microfluidic Device

Poornapriya Ramamurthy,[1,2] Joshua B. White,[1] Joong Yull Park,[3] Richard I. Hume,[4,5] Fumi Ebisu,[2] Flor Mendez,[2] Shuichi Takayama,[1] and Kate F. Barald[1,2,5]*

[1]Department of Biomedical Engineering, College of Engineering, University of Michigan, Ann Arbor, Michigan
[2]Department of Cell and Developmental Biology, University of Michigan Medical School, Ann Arbor, Michigan
[3]School of Mechanical Engineering, College of Engineering, Chung-Ang University, Seoul, Republic of Korea
[4]Department of Molecular, Cellular, and Developmental Biology, University of Michigan, Ann Arbor, Michigan
[5]Neuroscience Graduate Program, University of Michigan, Ann Arbor, Michigan

Background: To send meaningful information to the brain, an inner ear cochlear implant (CI) must become closely coupled to as large and healthy a population of remaining spiral ganglion neurons (SGN) as possible. Inner ear gangliogenesis depends on macrophage migration inhibitory factor (MIF), a directionally attractant neurotrophic cytokine made by both Schwann and supporting cells (Bank et al., 2012). MIF-induced mouse embryonic stem cell (mESC)-derived "neurons" could potentially substitute for lost or damaged SGN. mESC-derived "Schwann cells" produce MIF, as do all Schwann cells (Huang et al., 2002a; Roth et al., 2007; Roth et al., 2008) and could attract SGN to a "cell-coated" implant. **Results:** Neuron- and Schwann cell–like cells were produced from a common population of mESCs in an ultra-slow-flow microfluidic device. As the populations interacted, "neurons" grew over the "Schwann cell" lawn, and early events in myelination were documented. Blocking MIF on the Schwann cell side greatly reduced directional neurite outgrowth. MIF-expressing "Schwann cells" were used to coat a CI: Mouse SGN and MIF-induced "neurons" grew directionally to the CI and to a wild-type but not MIF-knockout organ of Corti explant. **Conclusions:** Two novel stem cell–based approaches for treating the problem of sensorineural hearing loss are described. *Developmental Dynamics 246:7–27, 2017*. © 2016 Wiley Periodicals, Inc.

Key words: stem cells; inner ear neurons; Schwann cells; deafness; microfluidics; myelination; cochlear implant

Submitted 1 February 2016; First Decision 16 September 2016; Accepted 30 September 2016; Published online 19 October 2016

Introduction

Development of new stem cell–based therapeutic approaches is bringing the era of regenerative medicine into more immediate focus. For example, a current area of intense interest to neuroscientists and bioengineers is the potential replacement of lost or diseased central and peripheral neurons and/or peripheral nervous system Schwann cells with biologically engineered stem cells. Ideally, stem cells would be capable of taking on the mature properties of both neuronal and Schwann cell types and could also participate in the critical cross talk that leads to myelination of the neurons by Schwann cells.

The inner ear's spiral ganglion's myelinated bipolar neurons (SGNs) provide the conduit for sensory messages from peripheral sensory receptors of mechanosensory hair cells to the central neurons in auditory brain stem nuclei. When the hair cells in the organ of Corti are lost or incapacitated, due to injury, aging, or loss of function resulting from genetic disorders, SGNs lose their peripheral targets and can progressively degenerate, so that the remaining neurons are less capable of functional interaction with either the remaining sensory organ of Corti hair cells or with a cochlear implant/prosthesis (Pfingst et al., 2015, review). Although SGN loss in humans is less pronounced than in animal models of hair cell loss or knockout mouse models of hair cell loss (Bermingham-McDonogh and Rubel, 2003; Bodmer, 2008; Breuskin et al., 2008), it appears that even if SGNs remain as long as 40 years post-onset of deafness, their functionality can be impaired (Sato et al., 2006; Wise et al., 2010; Jiang et al., 2006).

Dr. Poornapriya Ramamurthy's present address is Roche Diagnostics Clinical Operations (Study Manager), 79 TW Alexander Drive, 4401 Research Commons, Bldg./Suite 300, Durham, NC 27709
Dr. Fumi Ebisu's present address is Division of Protein Chemistry, Institute for Protein Research, Osaka University, Osaka 565-0871, Japan
*Correspondence to: Kate F. Barald, Department of Cell and Developmental Biology, Department of Biomedical Engineering, 3053 BSRB, 109 Zina Pitcher Place, Ann Arbor, MI 48109-2200; 734-647-3376. E-mail: kfbarald@umich.edu

Article is online at: http://onlinelibrary.wiley.com/doi/10.1002/dvdy.24466/abstract

In order to interact productively with a cochlear implant, the surviving SGNs must be healthy and sufficiently well distributed along the cochlea to cover the range of frequency distribution required to deliver the necessary information for speech discrimination (Parkins, 1985). Although conductive hearing loss can be remediated by using hearing aids, middle ear implants, and bone-anchored hearing aids, a direct stimulation of the auditory nerve is required when sensorineural hearing loss is severe. Such stimulation can be achieved by implanting cochlear prostheses/implants in the scala tympani of the cochlea. However, in the future, direct auditory brain stem implants may well become the standard therapeutic approach (reviewed in Merkus et al, 2014).

Some very promising studies of hearing restoration have recently been done in mammalian animal models. Endogenous supporting cells of the inner ear have been shown to differentiate and replace hair cell function (Mellado Lagarde et al., 2014; Wan et al., 2013; Monzack and Cunningham 2014, review). Human inner ear stem cells transplanted into deafened animal models also restored hearing function (Chen et al., 2012).

Strategies for prolonging survival or regenerating SGNs, many focused on earlier-identified inner ear neurotrophins as inducing agents (Roehm and Hansen, 2005; Ramekers et al., 2012), have been a focus of research for many years. To restore hearing function and prolong survival of existing SGNs, some researchers have developed paradigms in which a single neurotrophin or a cocktail of neurotrophins was administered to deafened animals using mini osmotic pumps or via cochlear implants coated with various gels/hydrogels that can slowly release such neurotrophins (Winter et al., 2007; Jun et al., 2008; Winter et al., 2008; Jhaveri et al., 2009). However, such treatment options have not yet progressed to clinical or even preclinical trials in patients with hearing loss (Miller et al., 2002; Pettingill et al., 2007; O'Leary et al., 2009; Pfingst et al., 2015).

To improve the performance of cochlear implants, a variety of different strategies to improve hearing perception are being tested, including advanced engineering of cochlear implant devices, which can communicate well with the brain stem (Pfingst et al., 2015, review); cell-replacement therapies, involving various types of stem cells to augment or substitute for lost or malfunctioning neurons (Corrales et al, 2006; Coleman et al., 2007: Reyes et al., 2008; Chen et al., 2012); regrowing spiral ganglion neuronal processes to improve connections with the implant and concomitantly reduce the distance between them (Altschuler et al., 1999); "classical" neurotrophin-releasing Schwann cells used to "coat" cochlear implants have been shown to enhance neurite contacts with the devices (O'Leary et al., 2009).

The research described in this report focuses on two stem cell–based strategies to address sensorineural hearing loss: replacement of damaged or lost SGNs, and neurotrophic factor-producing cells that could enhance the attractive properties of a cochlear implant. We used a microfluidic device with very slow differential flow (Park et al., 2009) to differentiate **a common population of embryonic stem cells** into two different types of cells, neuron-like cells and Schwann cell–like cells, using differential flow to deliver inducing agents for neurons and Schwann cells simultaneously in two streams of fluid, which, although side by side, move at different flow rates.

When macrophage migration inhibitory factor (MIF)—and not nerve growth factor (NGF) or ciliary neurotrophic factor (CNTF)—is the neuron-inducing agent, we show that the neuron-like cells bear some significant resemblance to statoacoustic ganglion or SGNs of the inner ear. NGF and CNTF also induce neuronal phenotypes: We have shown in other studies that NGF produces dorsal root ganglion–like neurons and CNTF induced motor neuron–like neurons (Roth et al., 2007; Roth et al., 2008; Bank et al., 2012). We have previously shown that MIF is the inner ear's first developmentally important neurotrophin (Holmes et al., 2011; Shen et al., 2012; Bank et al., 2012, cited in Faculty of 1000) and that receptors for MIF remain on SGNs into adulthood (Bank et al, 2012). These earlier studies were done in conventional tissue culture devices/dishes.

In this study, the MIF-induced neuron-like cells produced on the "neuronal" differentiation side of the slow-flow microfluidic devices were characterized for electrophysiological functional maturation by patch clamping, and for transporters, neurotransmitters, and appropriate ion channel expression by immunocytochemistry and RTqPCR. The MIF-induced neuron-like cells' properties were compared to the neuron-like cells induced with NGF or CNTF as we had done previously in our conventional tissue culture studies (Roth et al., 2007; Roth et al., 2008; Bank et al., 2012). The neuron-like cells' maturation is enhanced by exposure to docosahexaenoic acid (DHA), which is capable of enhancing both electrophysiological functional maturation (Uauy et al., 2001; Khedr et al., 2004) and myelination in the microfluidic device (Fig. 4).

Neuregulin (Gambarotta et al., 2013) was used to induce Schwann cell–like cells as in our previous studies (Roth et al., 2007; Roth et al., 2008) in the other fluid stream of the device. Our laboratory made the first embryonic stem cell–derived Schwann cells almost a decade ago (Roth et al., 2007). We demonstrated previously that these engineered Schwann cells have all the properties of myelinating Schwann cells (Roth et al., 2007), acquire Schwann cell–like properties in the expected order during maturation, and produce MIF as do all vertebrate Schwann cells (Huang et al., 2002a).

Such stem cell–derived neuron-like and Schwann cell–like cells could be used independently or together to provide therapeutic approaches to alleviate a variety of neurological disorders, including multiple sclerosis (Taupin, 2011; Zhang et al., 2011), spinal cord injury (Paino et al., 1994; Goodman et al., 2007; Zhang et al., 2007; Boomkamp et al., 2012), Parkinsonism (Mena and Garcia de Yebenes, 2008), peripheral nerve regeneration (Namqung et al., 2015), and, most important for these studies, **sensorineural hearing loss/deafness** (Pettingill et al., 2008). Replacement of the sensory hair cell population from stem cells endogenous to the inner ear is also under investigation (Li et al., 2003a,b; Liu et al, 2014), although not in these studies.

It has been difficult to study the stages of neuron–Schwann cell interactions that result in myelination in conventional tissue cultures of primary peripheral system neurons and Schwann cells (Gingras et al., 2008; Heinen et al., 2008; Callizot et al., 2011; Jarjour et al., 2012) for several reasons: The inability to distinguish **living** primary neurons from Schwann cells in conventional cell co-cultures during the differentiation and interaction processes (Paivalainen et al., 2008), unless one population or the other is tagged with a live cell label; the difficulty in obtaining immature cultures of both primary neurons and Schwann cells in order to observe and document the key *early* steps in their interactions that lead to myelination; and sufficiently specific stage-specific markers of myelination progress, as our earlier studies documented (Roth et al., 2007; Roth et al., 2008).

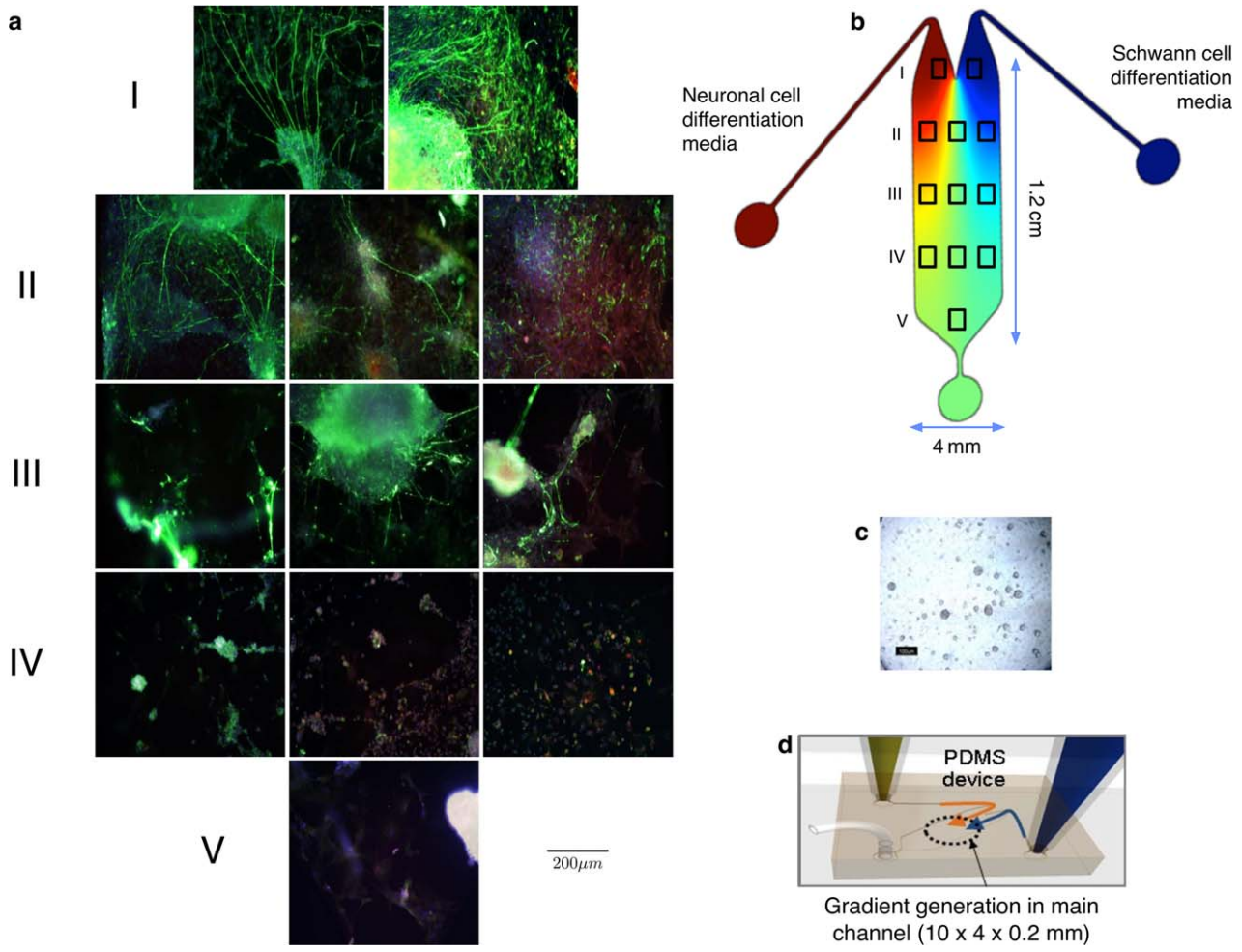

Fig. 1. The mouse embryonic stem cells (mESC) seeded on the device differentiated into both neuron-like and Schwann cell–like cells. (**a**) Photomigrographs of the areas of the device depicted as boxes in the cartoon (**b**) were taken after the whole device was stained for Neurofilament 150kDa, neurites (green); DAPI, nucleus (blue); MPB, evidence of Schwann cell myelination (red). After three weeks, the top three rows (I, II, III) show significant neuronal differentiation as well as directional outgrowth of neurites (green) toward the "Schwann cell" sectors (those on the right). In the bottom two rows (those with the most media intermixing and least preserved gradients), the cells apparently did not differentiate into any specific lineage (IV and V). The white arrows in (a) indicate the directional outgrowth of neurites. (**c**) Undifferentiated mES cells in the microfluidic device. (**d**) A cartoon of the microfluidic device. The gradient flow illustration (b) and microfluidic chip channel dimensions (d) are adapted from Park et al., 2009.

Tissue engineered co-culture systems have been somewhat successful in identifying key molecular steps and markers in studies of myelination (Hsu and Ni, 2009; Liazoghli et al., 2012). A number of such co-culture systems have involved variously derived stem cells (Yang et al., 2008: Wei et al., 2010; Xiong et al., 2012; Yang et al., 2012), mostly to provide the "neuronal" component. However, none of these engineered stem cell–based systems has been sufficient to observe the continuum of cell-cell interactions that result in early events in myelination.

The very slow-flow devices used in these studies allow us to study neuronal/Schwann cell interactions that result in onset of myelination during the course of the experiment, which can be carried out for up to six weeks. An osmotic pump is essential to achieving sufficiently slow flow with low shear that does not cause cell detachment and that allows us to culture cells in devices with nutrient replenishment and eliminate wastes for up to six weeks.

The device was designed to generate overlapping gradients of one of the neurotrophic factors (MIF, NGF, or CNTF) (Bank et al., 2012) as well as Schwann cell–inducing factors (Neuregulin) (Roth et al., 2007), from two different inlets (Fig. 1, cartoon). By stably maintaining flow over a three- to six-week period, we were able to correlate cell differentiation and neuronal outgrowth to computed concentrations of the different factors, and to document many aspects of the interactions between the two cell types in the device, particularly the very early events in myelination. The microfluidic device allows us to study the cell-cell interactions between the "neurons" and the "Schwann cells" with time-lapse digital cinematography, and also permits molecular, immunohistological, and electrophysiological analyses of the cells in the device itself.

The role of MIF produced by the "Schwann cells" in promoting directional outgrowth of processes from the "neurons" toward the Schwann cell side of the device was tested in two ways. After the embryonic stem cells had differentiated into "Schwann cells" or "neurons," we blocked MIF production on the Schwann cell side of the device with the biochemical MIF inhibitor 4-iodo-6-phenylpyrimidine (4-IPP) at 0.1 μM 4-IPP for seven days, as we

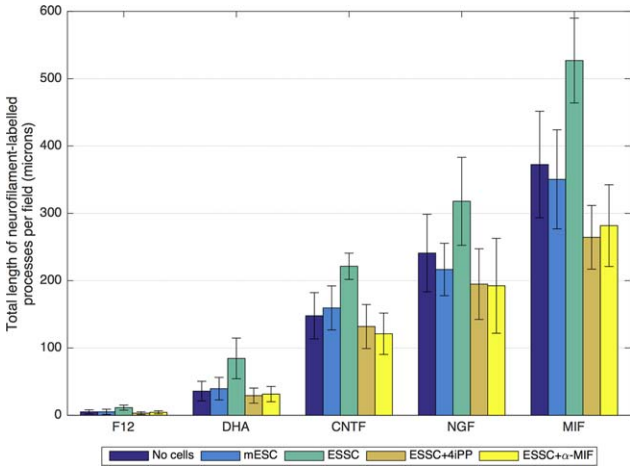

Fig. 2. Neurite measurements of the neuron-like cells differentiated with different neurotrophic factors with and without DHA in the microfluidic device. The "neurites" of neuron-like cells co-cultured with Schwann cell–like cells in the microfluidic device grew directionally toward and over the "Schwann cell" lawn. Total process lengths were measured using MetaMorph or ImageJ software for this directional outgrowth; eight experiments using a minimum of 10 photographed fields of view in each were used.
mESC = undifferentiated mouse embryonic (D3) stem cells on the "Schwann cell" side of the device. ESSC = Embryonic stem cell–derived Schwann cells; these are Neuregulin-induced "Schwann cells" derived from the mESC. ESSC + 4iPP: Under these conditions, the differentiated "Schwann cell" lawns on the Schwann cell side of the device were treated with the biochemical MIF inhibitor 4iPP (as described in Experimental Procedures and in Shen et al., 2012). ESSC + α-MIF: Downstream MIF effects were blocked by addition of a function-blocking anti-MIF antibody (α-MIF), as we had done in previous studies (Bank et al., 2012).
Significance Calculations for These Data
Differences between treatment groups and statistical significance were analyzed using Mann-Whitney U-tests performed in MATLAB. There were statistically significant differences found among these treatment groups with P values as indicated below:
DHA alone: mESC vs. ESSC, $P = 0.0023$; ESSC+4iPP vs. ESSC, $P = 3.1080 \times 10^{-4}$; ESSC + α-MIF vs. ESSC, $P = 5.4390 \times 10^{-4}$
CNTF alone: mESC vs. ESSC, $P = 1.5540 \times 10^{-4}$; ESSC+4iPP vs. ESSC, $P = 7.7700 \times 10^{-5}$; ESSC + α-MIF vs. ESSC, $p = 7.7700 \times 10^{-5}$
NGF alone: mESC vs. ESSC, $P = 0.0050$; ESSC+4iPP vs. ESSC, $P = 0.0015$; ESSC + α-MIF vs. ESSC, $P = 0.0052$
MIF alone: mESC vs. ESSC, $P = 5.4390 \times 10^{-4}$; ESSC+4iPP vs. ESSC, $P = 7.7700 \times 10^{-5}$; ESSC + α-MIF vs. ESSC, $P = 7.7700 \times 10^{-5}$

have done previously (Shen et al., 2012). In another set of experiments, we blocked MIF downstream pathways with a monoclonal antibody to MIF using conditions we previously established for studies of both mouse- and chick-cultured primary neurons and stem cell–derived neurons (Bank et al., 2012). Blocking MIF resulted in a significant reduction in directional neurite outgrowth toward the "Schwann cell" lawn in the microfluidic devices (Fig. 2), just as we previously demonstrated in conventional tissue culture experiments (Bank et al., 2012).

Once we had convincing data confirming our earlier studies that MIF appears to be involved in directional neurite outgrowth either through its direct effects (see Fig. 1 in Bank et al., 2012) or through its production by a mouse embryonic stem cell (mESC)-derived "Schwann cell" lawn (see Fig. 5B in Roth et al., 2007), we used the MIF-producing mESC-derived Schwann cells, encapsulated in sodium alginate hydrogels, to coat two types of cochlear implants: the multi-electrode type commonly used in human patients and the simple ball type used in animal studies.

Directional outgrowth of neurites from primary mouse statoacoustic ganglion (which is the embryonic precursor of both the spiral ganglion [SG] and the vestibular ganglion [VG] in vertebrates that develop both SG and VG) and spiral ganglion explants extending neurites toward the devices was observed by time-lapse cinematography. Contacts with the implants were visualized by immunocytochemistry using specific markers.

MIF-induced neuron-like cells were also co-cultured with mouse organ of Corti explants, and directional outgrowth of neurites toward the target was documented toward wild-type but not the MIF-knockout organ of Corti explants. We had already demonstrated that this could be done with primary neurons in conventional tissue culture (Bank et al., 2012).

This study could eventually benefit two types of patients: those with low SGN counts who are not good candidates for cochlear implant therapy, for whom a replacement population of stem cell–derived neuron-like exogenous cells could enhance functional contacts with their own native organ of Corti sensory hair cells; and those for whom cochlear implants coated with MIF-producing Schwann cell–like cells could markedly improve directional outgrowth of their remaining SG neurites to the cochlear implant.

Results

Concomitant Differentiation of mESCs into Neuron-like Cells and Schwann Cell–like Cells in a Slow-flow Microfluidic Device

We differentiated mESCs into both neuron-like cells and Schwann cell–like cells in the same microfluidic device to study cell differentiation and maturation (neuronal or Schwann cell), as well as any cell-cell interactions between the Schwann cells and the neurites emerging from the neuron-like cells, e.g., those that might result in evidence of myelination by the Schwann cell–like cells.

The microfluidic system was designed to establish a gradient flow to nourish the stem cells with nutrients and growth factors or neurotrophic cytokines in order to facilitate the differentiation of two different cell populations from a single undifferentiated stem cell population seeded on the device. Figure 1C is a bright-field image of undifferentiated mESC (Doetschman et al., 1985) seeded over the entire surface area of the device after coating the device with sterile porcine gel (see Experimental Procedures). A cartoon of the device, with the "neuron" side depicted in red and the "Schwann cell" side depicted in blue, is seen in Figure 1B. Then, using differential flow, Schwann cell–like cells were induced to form on the right half of the device (blue outflow source seen in the cartoon in Fig. 1B,D) using concentrations of Neuregulin that we had previously determined produced myelinating Schwann cells (Roth et al., 2007; Roth et al., 2008).

One of three different inducing agents was used to produce the neuron-like cells in the left (Fig. 1B, red) half of the device: NGF, CNTF, or MIF at concentrations we had previously optimized (Roth et al., 2007; Roth et al., 2008; Bank et al., 2012; see Experimental Procedures). The "neuron"-inducing agent was delivered from the reservoir indicated in red in the cartoon in Fig.1B,D. DHA enhancement was also tested in the microfluidic devices in some cases, and it was delivered through the same portal. DHA enhancement had proven to be very effective in our previous studies, even at the lowest concentration we tested (Bank et al.,

2012). Three to eight duplicate devices for each inducing agent or condition were prepared in parallel, incubated, fixed, labeled (e.g., with antibodies to Neurofilament [NF] or TUJ1), photographed, and analyzed for each set of conditions using MetaMorph software.

After one week in the microfluidic devices, we saw both morphological and molecular evidence of neuronal differentiation on the "neuronal" side of the device under all neuron-inducing conditions at the concentrations tested (see Experimental Procedures), including DHA alone. Neurofilament-positive cell bodies with extensive processes were documented photographically and analyzed by MetaMorph or NIH ImageJ software. By contrast, little if any neuronal differentiation was seen at one week in the presence of F12 medium alone (control) (Fig. 2), as we had also previously documented (Roth et al., 2007; Roth et al., 2008; Bank et al., 2012).

After two to three weeks, we observed that more than 75% of the mESCs exhibited neuronal processes in response to NGF, CNTF, or MIF, as well as to any of these inducing agents enhanced with DHA. However, because the "neuron-like" cells were clumped together and the processes were found in fascicular bundles (e.g., Bank et al., 2012, Fig. 2), it was often difficult to determine the actual numbers of neuron-like cell bodies in the clumps or how many processes were present in the fascicles. Fasciculation was enhanced markedly by the addition of DHA.

Directional Neurite Outgrowth is Observed from the Neuron-like cells Toward the "Schwann cell" Sectors in Microfluidic Devices

To determine if there was preferential neurite outgrowth from the neuron-like cells toward the Schwann cell–like cells in the microfluidic device (Fig. 1A), we used time-lapse videomicrography and end-stage photomicrography to identify immunolabeled (Neurofilament or TUJ1) cells and processes on the "Schwann cell" side of the devices. Photographs of the immunolabeled cells were analyzed by MetaMorph or NIH ImageJ software. For these analyses, we virtually sectioned the device into five rows (Fig. 1A,B; I, II, III, IV, V). Rows II, III, and IV were divided into three columns for taking the photomicrographs used in these analyses (Fig. 1B, cartoon). The mESC showed concentration-dependent differentiation from the channel inlet to the outflow port (Fig. 1B, cartoon) as a round green area at the bottom. ESCs took on neuronal morphologies in areas closest to the left inlet (Fig 1A; I, II). The cells that became neuron-like in sectors I and II, and any found in III, extended neurites toward the Schwann cell–like cell lawns (e.g., Fig. 1A; I, right image), since Schwann cell–like cells produce MIF, which is both a neurite outgrowth and survival factor for many different neuronal subtypes, including those in the inner ear (Bank et al., 2012) and eye (Ito et al., 2008). We tested the role of MIF directly in additional studies (Fig. 2). The extension of ramifying processes of the neuron-like cells over the Schwann cell lawn is also typical of the behavior of primary neurons on such engineered Schwann cell lawns (see Fig 5B in Roth et al., 2007). Neurofilament-positive neuron-like cells that differentiated in Row III (Fig. 1A; III, middle) had minimal numbers of neuronal processes; however, the few processes that were present grew directionally toward the Schwann cell lawn (Fig. 1A,B, blue side of the device). Neuron-like cells in Row IV also could be labeled for Neurofilament but no processes developed in this region (Fig. 1A; IV). There were cells in Row IV that were not stained for Neurofilament (Fig. 1A) but could be stained for myelin basic protein (MBP), indicating that they were "Schwann cells" (see also Fig. 4), as in our previous work (Roth et al., 2008). Cells in Region V did not express markers for either Schwann cells or neurons, nor was there evidence of myelination, indicating the undifferentiated ES status of these cells, many of which still expressed Oct4 (Roth et al., 2007; Roth et al., 2008; Bank et al., 2012), a marker for undifferentiated stem cells (Pan et al., 2002). The gradient profile created in the device, in which the highest concentrations of neuron-inducing and Schwann cell–inducing media predominated near the inlets, facilitates ES cells' differentiation into neuron-like cells and Schwann cell–like cells with a much higher expression level of their cell type specific protein markers (Fig. 1A; I, II, III). Neurites extending over the Schwann cell lawn in Row I (Fig. 1A; I, right image) also exhibited the most neurite fasciculation compared with the other sections of the device. We observed cell differentiation by both time-lapse cinematography and end-stage photomicrography. We measured the total neurite outgrowth of the processes using confocal microscopy and light photomicrography, analyzed by MetaMorph software or NIH ImageJ software (see Experimental Procedures).

MIF Production by Schwann Cell–like Cells Appears to Play a Role in Directional Process Outgrowth

When devices were stained with an antibody to Neurofilament and appropriate secondary antibodies, little or no directional outgrowth toward the "Schwann cell" side of the device was seen under any of the "neuron-inducing" conditions (Fig. 2) if there were no cells on the "Schwann cell" side of the device. This was also the case if there were undifferentiated mESCs (not exposed to Neuregulin) on the "Schwann cell" side. However, if Neuregulin had been used to induce a Schwann cell–like phenotype, there was a significant **directional** process outgrowth toward the Schwann cell lawns (Fig. 2). Compare the process outgrowth toward the undifferentiated mESC lawns with outgrowth toward mESCs induced to become Schwann cell–like with Neuregulin ESSC (Fig. 2). mES–Schwann cell differentiation resulted in ramification of "neuron-like" processes over the Schwann cell lawns, no matter *which* neuronal inducing agent was used on the "neuron" side (see Fig. 5B in Roth et al., 2007). However, more extensive process outgrowth and more extensive fasciculation were seen if the inducing agent was MIF (Fig. 2), and the difference was significant (compare the statistics for the various neurotrophic inducing agents included in the caption to Fig. 2).

As we had demonstrated in our previous studies (Roth et al., 2007; Bank et al., 2012), MIF production by the differentiated Schwann cell–like cells induced by Neuregulin appears to provide a major impetus for this process extension, whether by primary neurons (Fig. 5B; in Roth et al., 2007) or stem cell–derived "neurons" (Fig. 2). We examined this directly by blocking MIF downstream effects in one of two ways: 1) The biochemical MIF inhibitor 4-IPP at a final concentration of 0.1 μM, was used as described previously (Shen et al., 2012); or 2) a MIF function-blocking monoclonal antibody, also used as described previously (Bank et al., 2012). These MIF-blocking strategies were used *only* on the Schwann cell side of the device (Fig. 1, in blue in the cartoon) once both cell types ("neuron-like" and "Schwann cell–like") had phenotypically differentiated. Use of either means of

TABLE 1. Primer Pairs for Assessing General and Inner Ear–Specific Neuronal Differentiation

Undifferentiated cell marker	OCT4		
Early-stage neuronal markers	Neurogenin1(Ngn1)	GAGCCGGCTGACAATACAAT	AAAGTACCCTCCAGTCCAG
	NeuroD	AGGCTCCAGGGTTATGAGAT	TGTTCCTCGTCCTGAGAACT
	Neurofilament	GGAATTCGCCAGTTTCCTGA	GCAAGGTTCTCCCATGAACA
Mature neuronal markers	Neurotrophic tyrosine kinase receptor type 2 (TrkB)	ACCATAAACCACGGCATGAG	CCGTGAAGCAGAGTTCAACA
	Neurotrophic tyrosine kinase receptor type 3 (TrkC)	AACCATCACGAGAAAGCCTG	ACCATCTCCACCTCTGCTTA
	Peripherin (Prph)	TCGACAGCTGAAGGAAGAGA	AGAGGCAAAGGAATGAACCG
Auditory neuronal markers	Gamma-aminobutyric acid A receptor (GABA-AR)	TCATCCTCAACGCCATGAAC	TCACCTCTCTGCTGTCTTGA
	Vesicular glutamate transporter 1 (VgluT1)	CCAAGCTCATGAACCCTGTT	ACCTTGCTGATCTCAAAGCC
	Voltage-gated sodium ion channel (SP19 orNAV1.1)	CCATGATGGTGGAAACGGAT	AGATGAGCTTGAGCACACAC

inhibiting MIF downstream effects reduced the extent of "neurite" outgrowth over the "Schwann cell" lawns to levels seen when either no cells or undifferentiated mESCs (no Neuregulin) were plated on the "Schwann cell" side of the device. This difference was particularly large and significant for the MIF-induced "neurons" (Fig. 2; significance calculations in the caption).

In summary, for "neurons" induced by DHA alone and by each neurotrophin (CNTF, NGF, and MIF), the ESSC condition has a significantly higher mean value for directional neurite outgrowth than the mESC, ESSC+4iPP, and α-MIF conditions. This is not surprising since all Schwann cells are known to produce MIF (Huang et al., 2002a; Huang et al., 2002b; Nishio et al., 2002; Bank et al., 2012) as well as another neurotrophic cytokine, monocyte chemoattractant protein 1 (Bianchi et al., 2005; Roth et al., 2007; Roth et al., 2008; Bank et al., 2012). Furthermore, vertebrate statoacoustic ganglion neurons, SGNs, and MIF-induced stem cell–derived neurons are known to express MIF receptors (Shen et al., 2012; Bank et al., 2012) and to continue to express these receptors into adulthood (Bank et al., 2012). We have shown that MIF is a *directional* neurite outgrowth factor for many neuronal subtypes, particularly those in the inner ear (Roth et al., 2007). We have also shown that it is a neuronal survival factor (Bank et al., 2012).

Neuron-like Cells in the Microfluidic Devices Develop Neuronal Characteristics as Assessed by Appearance of Neuronal Markers Measured with RTqPCR

Analysis of neuronal differentiation using primer pairs (Table 1) for neuronal markers and for undifferentiated ES cells (Oct4 expression; Pan et al., 2002) was done by RTqPCR, as in our previous studies (Roth et al., 2007; Roth et al., 2008; Bank et al., 2012). Oct4 remained at high expression levels under proliferative conditions (no neuronal differentiation media added) and was down-regulated under differentiation conditions (Fig. 3A). Cells treated with cytokines or neurotrophins alone showed a two-fold down-regulation of Oct4 gene expression and cells treated with DHA as well as MIF, and/or neurotrophins showed a four-fold Oct4 down-regulation when compared with the undifferentiated conditions (Fig. 3A).

In general, neurotrophins (Flores-Otero et al. 2007; Bank et al., 2012) are thought to provide molecular signals that mediate the survival of neurons. In mice, ganglion neuron precursors and developing cochlear neurons express the proneural gene Ngn-1. NeuroD and NF are up-regulated early in inner ear development (Flores-Otero et al. 2007; Nayagam et al., 2011; Yang et al., 2011; Shibata et al., 2011: Reyes et al., 2008). In SGNs, three different forms of Nfil are expressed sequentially (Nayagam et al., 2011; Yang et al., 2011). In these studies, we found Ngn-1 expression was up-regulated under all neuronal differentiation conditions when compared with cells grown in F12 basal media (undifferentiated conditions) (Fig. 3B). Expression of NeuroD was up-regulated in cells treated with MIF alone, with CNTF+DHA, NGF+DHA, and MIF+DHA (Fig. 3B). A rise in NeuroD expression levels suggests that MIF alone without DHA could support the differentiation and survival of stem cell–derived neurons. CNTF, MIF, CNTF+DHA, NGF+DHA, and MIF+DHA significantly increased NeuroD expression when compared with mESCs grown in the F12 basal medium.

Nfil expression was up-regulated significantly under all the differentiation conditions compared with F12 basal medium. Nfil expression was up-regulated in cells treated with CNTF+DHA, NGF+DHA, and MIF+DHA when compared with conditions without DHA (Fig. 3B). Proneural gene marker up-regulation in cells treated with MIF alone and MIF+DHA suggests that the

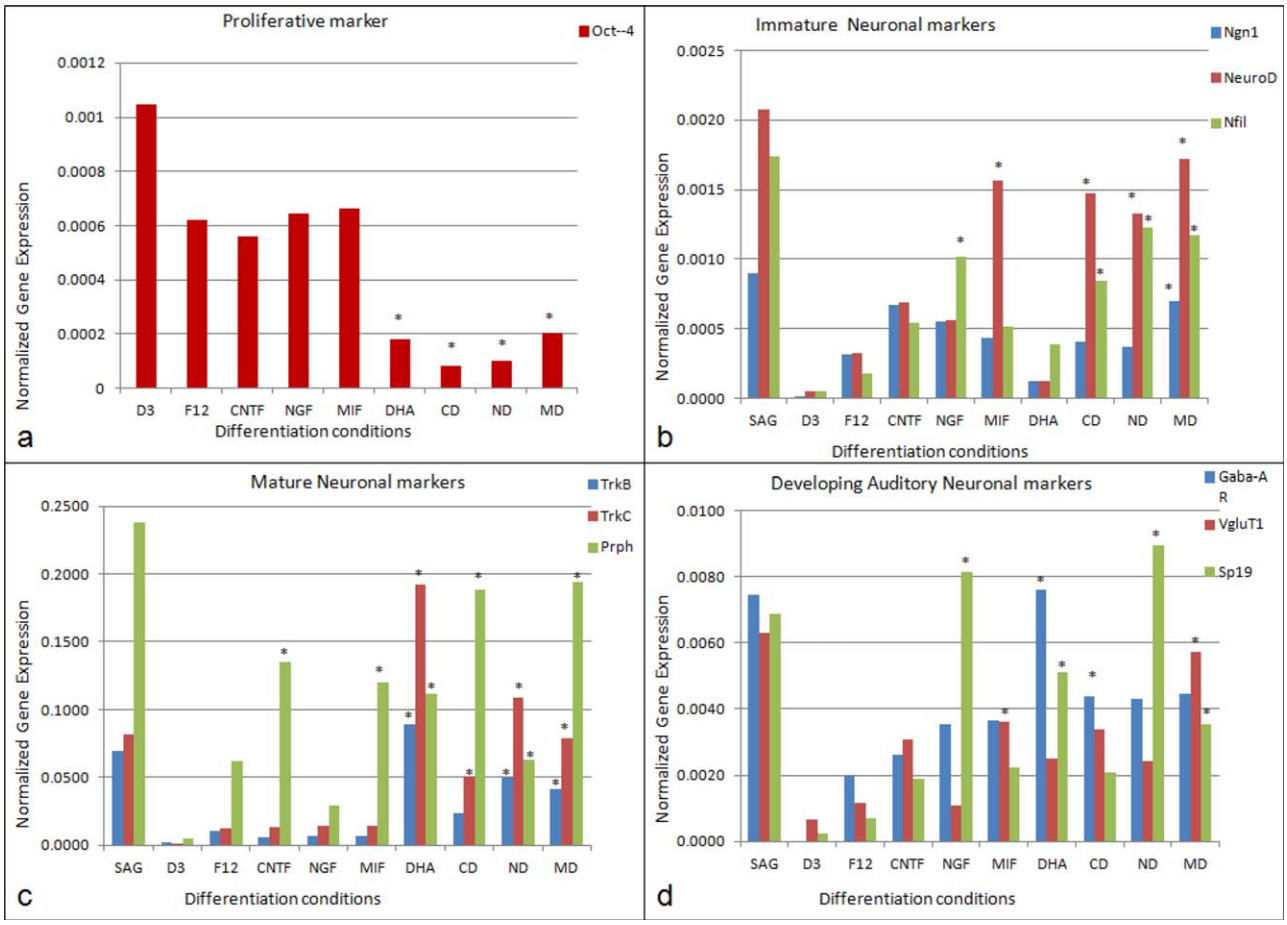

Fig. 3. RTqPCR quantification of gene marker expression in the differentiated neuron-like cells (**a**) OCT4 expression in undifferentiated mES cells and neuron-like cells differentiated from mES cells. D3: Undifferentiated condition, statoacoustic ganglion: (SAG) spiral ganglion neuron culture (control). (**b**) Expression of proneural marker genes in neuron-like cells. Ngn-1, NeuroD, and Nfil (NF) expression is much higher in neuronally differentiated cells, but not detected in undifferentiated condition (D3ES). (**c**) Expression of mature neuronal marker genes: TrkB, TrkC, and Prph in the neuron-like cells are up-regulated in all the neuronal-differentiated conditions, and expression levels are much higher under conditions with DHA addition. F12, neuronal basal media; C, CNTF differentiation condition; N, NGF differentiation condition; M, MIF differentiation condition; D, DHA differentiation condition; CD, CNTF+DHA differentiation condition; ND, NGF+DHA differentiation condition; MD, MIF+DHA differentiation condition. (**d**) Expression of auditory neuronal markers: GABA-AR, VgluT1, and SP19 are highly up-regulated in the neuronal differentiation conditions compared to undifferentiated conditions and F12 (basal) medium. VgluT1 expression is much higher in the MIF+DHA condition than in all the other differentiation conditions, which was to be expected given that MIF is the inner ear's first differentiation "neurotrophin" (Holmes et al., 2011; Bank et al. 2012; Shen et al., 2012).

cells' expression profile is consistent with what can be expected of expression in statoacoustic ganglion neurons (the spiral ganglion neuronal precursors) (Fig. 3B).

A number of transcription factors (GATA3, Brn3a, Ngn-1, NeuroD, islet1) as well as receptors for neurotrophins (TrkB and TrkC) have been defined as mature markers for differentiating auditory and vestibular neurons (Nayagam et al., 2011; Shibata et al., 2011; Yang et al., 2011). Peripherin (Prph) is also expressed concomitantly with axonal growth during development in the inner ear, and its synthesis appears necessary for axonal regeneration in the adult (Nayagam et al., 2011; Shibata et al., 2011; Yang et al., 2011). TrkB, TrkC, and Prph were significantly up-regulated under conditions of DHA supplementation of either of the two neurotrophins or MIF (Nayagam et al., 2011; Shibata et al., 2011; Yang et al., 2011). Up-regulation of these "mature" neuronal markers and some selected auditory system neuronal markers are seen in Figure. 3C,D.

Differentiated neuron-like cells were stained for VgluT1 (a marker for SGNs of the inner ear), Neurofilament 200 (NF200) (a neuronal marker), and MBP, which labels mature, neuron-interactive myelinating Schwann cells (Roth et al., 2007; Roth et al., 2008) (Figs. 1, 3). Differentiation conditions under which cells were treated with NGF, CNTF, or MIF, either of the neurotrophins+DHA, or MIF+DHA exhibited more extensive neurite outgrowth than was seen in the F12 basal medium. Differentiation conditions with neurotrophins or with MIF supplemented with DHA have extensive fasciculated bundles of neurites, which were positive for the glutamate transporter VgluT1 and Neurofilament (Nfil200kDa). By contrast, few neurites stained for both VgluT1 and Nfil200 under conditions in which CNTF, NGF, MIF, or DHA alone were used as the inducing agents. All the differentiated neuron-like cells in the mid-region of the device showed healthy neurite outgrowth over the lawn of Schwann cell–like cells, as did cells treated with CNTF+DHA, NGF+DHA, and MIF+DHA (see Fig. 2 for total neurite outgrowth measurements).

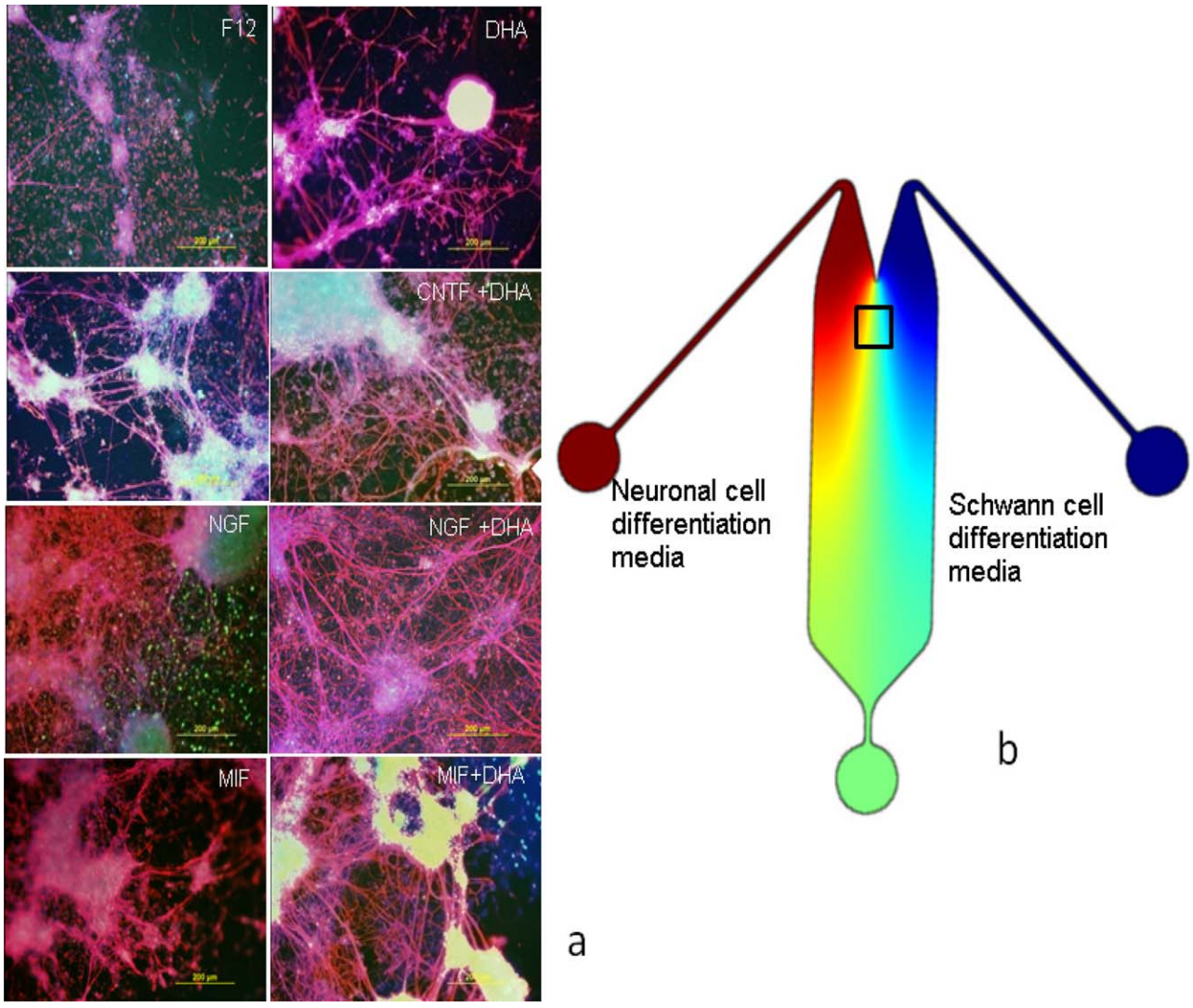

Fig. 4. Observations of myelination onset as neuron-like cells and Schwann cell–like cells interact in the midsection of the microfluidic device, Row II. The cultures were stained for Neurofilament-heavy 200kDa (NF-H) (red), myelin basic protein (blue), and VgluT1 (green). (**a**) Merged images of multi-labeled devices (**b**) Cartoon showing the location of Row II, which is also shown Fig. 1. F12, the basal medium; CNTF, ciliary neurotrophic factor; NGF, nerve growth factor; MIF, macrophage migration inhibitory factor; DHA, docosahexaenoic acid.

A substantial increase in glutamatergic properties (e.g., increased VgluT staining of neurites), robust neurite outgrowth with multiple branches, and evidence of myelination in the device were all found in MIF-induced neuron-like cells. Although these properties do not exclusively define SGNs, development of these properties indicates that the cells were developing at least some of the properties of SGNs. Such criteria would be critical if the "neuronal" population were to prove adequate substitutes for lost or diseased SGNs in vivo.

Evidence of Early Steps in Myelination is Seen in the Microfluidic Devices in CNTF and MIF-derived "Neurons"

If NGF was used as the inducing agent, little evidence of myelination was seen during the time course of these experiments (up to 30 days), even in the presence of DHA (NGF+DHA: Fig 4) or the presence of Schwann cell–like cells. However, neuron-like cells induced by CNTF showed evidence of myelination with and without DHA in the presence of Schwann cell–like cells. When neuron-like cells were induced with the neurotrophic cytokine MIF, the presence of DHA greatly enhanced evidence of myelination in the presence of the Schwann cell–like cells (Fig. 4).

The process of myelination is extremely difficult to follow at the cellular level in its entirely in (approximately) real time in vivo without sacrificing large numbers of animals. Even in vitro, using primary cell cultures of neurons and Schwann cells, the process is difficult to observe (Callizot et al, 2011). However, in the microfluidic device, we have created a microenvironment in which the cells can be differentiated concomitantly into the two lineages. We can now begin to study the interaction between the two cell types by time-lapse video and by stage-specific immunolabeling (Roth et al., 2007) as they mature and mutually influence the other population's development, as happens in vivo (Salzer, 2012; Salzer, 2015; Glenn and Talbot, 2013; Kidd et al., 2013). Schwann cell myelin production requires the influence of neurons capable of carrying on the complex sequence of required cell-cell interactions and molecular cross talk (Bodhireddy et al.,

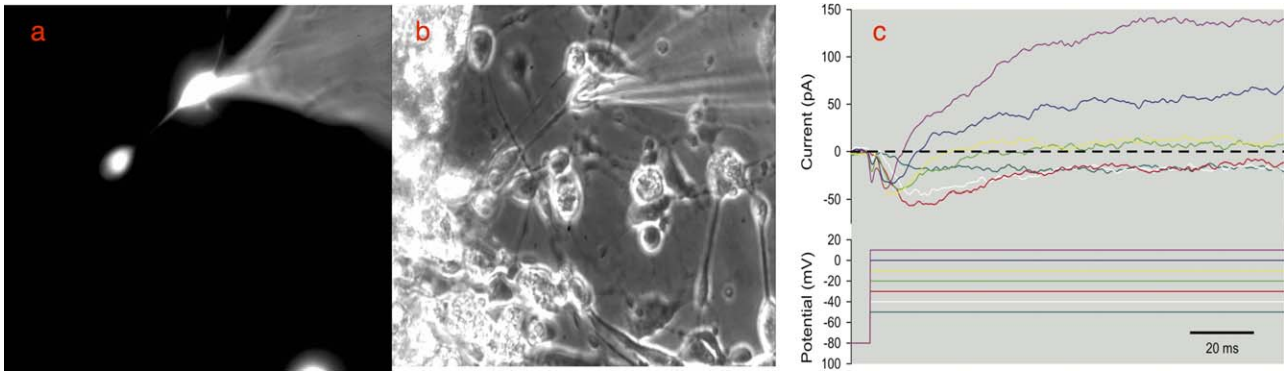

Fig. 5. Patch clamp studies performed on the neuron-like cells induced by MIF. (**a**) Electrodes were filled with ionic fluorescent rhodamine dye and used to patch-clamp the cell membrane of cells identified as having a neuronal morphology. (**b**) Phase-contrast image of a group of differentiated neuron-like cells; the cells that were identified as having a bipolar neuronal morphology were patch-clamped using a fire-polished glass pipette electrode. (**c**) MIF- and DHA-treated ES cells showed voltage-dependent inward and outward current with long active response times, demonstrating voltage-dependent currents in a neuron-like bipolar cell. Voltage-dependent changes were seen in response to step depolarization from a holding potential of -80 mV. Both transient inward currents and maintained outward currents were observed. The linear leak currents and most of the linear capacity currents were removed during data acquisition with a P/8 protocol (although a small residual-capacity transient is visible immediately after the voltage steps). The ionic conditions were set so that ENa and EK were at normal levels, and neither sodium nor potassium channels were blocked, so the responses to small voltage steps are dominated by transient inward sodium currents that got faster as the cell was depolarized, and the response to large steps was dominated by a maintained outward current.

1994; Roth et al., 2007; Salzer, 2012; Salzer, 2015). We had previously found evidence of early steps in myelination in interactions between primary inner ear statoacoustic ganglion neurons and a "Schwann cell" lawn produced by inducing the Schwann cell phenotype in ESCs (Roth et al., 2008).

Importantly, the slow-flow feature of our device, which closely approximates interstitial flow with respect to diffusion strength, is physiological for neuronal cells. Neurons usually develop in and remain separated from high-flow-rate environments (blood flow or even lymphatic flow in the body), which at least for the central nervous system (CNS), where oligodendrocytes and not Schwann cells myelinate neurons, is maintained by the blood-brain barrier. It is important to note that even in such flow-free environments, neurons still require a replenished nutrient supply and waste-clearing by minimal convective flow, which is also achieved in our slow-flow device. Stability of the flow in the channel is guaranteed since the operation of the flow is based simply on osmosis, a very stable phenomenon. The overall pattern of the two differentiated cell types in the device suggests that the neuron-like cells grown with the Schwann cell–like cells exhibited directional outgrowth toward the Schwann cell–like target cells (e.g., Fig. 1A; I, right image). This observation recapitulates our earlier finding that neurites from primary ganglionic explants similarly ramify over such a stem cell–derived Schwann cell lawn (Roth et al., 2007). There is ample evidence of the early stages of myelination (Fig. 4) as these differentiating "neurons" and "Schwann cells" interact.

Properties of Neuron-like Cells Differentiated by MIF or MIF+DHA Could Lend Themselves to Replacement Strategies for Inner Ear Neurons

We used whole-cell patch clamp electrophysiological recordings to determine whether the neuron-like cells derived from mESCs induced with MIF had excitable properties that showed voltage-gated inward and outward currents. This would be the minimum requirement for action potentials and therefore render these cells capable of encoding frequency information from a cochlear implant electrode and conveying it to the CNS. After three weeks, an excitable population of neuron-like cells was identified in the 80% of cells that had taken on a neuronal morphology. The population with measurable excitable properties was approximately 25% of the cells with a neuronal morphology. By contrast, if the mESCs were exposed to the F12 basal medium without any differentiation factors, no such properties could be documented.

To explore the underlying cause of these electrophysiological changes, we investigated the voltage-dependent properties of Na + and K + currents using whole-cell voltage-clamp electrophysiology. We detected voltage-dependent inward and outward current with long active response times in the MIF/DHA exposed "neurons" (Fig. 5C), whereas the cells in F12 media alone (basal medium) showed no neuronal morphology and no active responses or any inward or outward currents. Electrophysiological recordings were also made in the NGF+DHA condition. However, no inward or outward currents were found. We also labeled the MIF- and/or DHA-induced neuron-like cells for ion channel protein expression with antibodies for sodium ion channel SP19 and potassium ion channel Kv3.1 on the same cell preparation (double labeling). SP19 was distributed all over the somas and along the neurites, as well intracellularly (potentially nuclear staining); Kv3.1 was also expressed in the cell body and along the processes, although the staining was as well defined (data not shown). This finding does, however, agree with our RTqPCR data (Table 1).

Coating of SC Cells on Cochlear Implants Using Hydrogel Layering

Based on the preliminary analyses of MIF neuron-like cells that showed these cells had features that could potentially serve in the place of SGNs, we were sufficiently encouraged to proceed to "coating" CIs with MIF-producing Schwann cell–like cells. We then followed the interaction of the MIF-induced neuron-like cells with these "coated" implants in vitro. Earlier work by Shepherd's group (Pettingill et al., 2007) had demonstrated that CIs

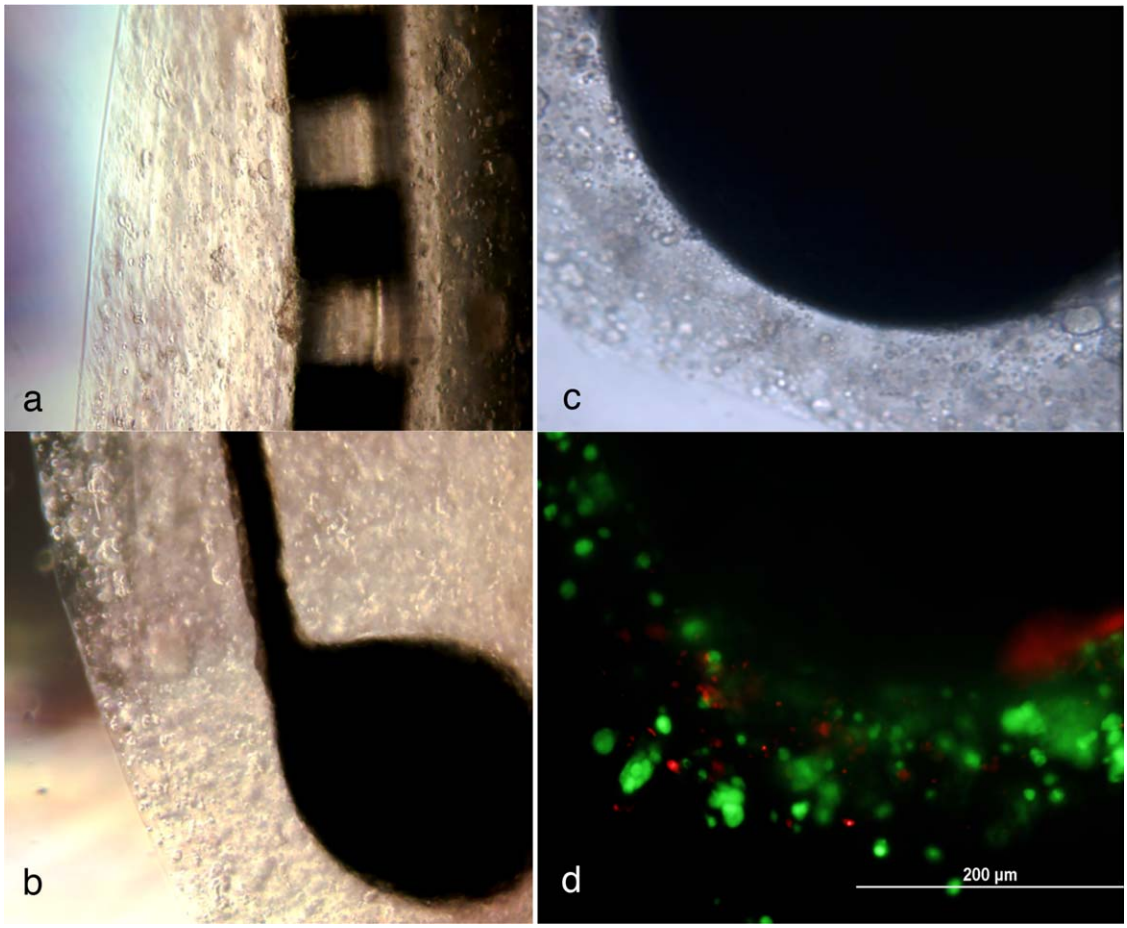

Fig. 6. Two types of CIs coated with hydrogels with encapsulated Schwann cell–like cells: (**a**) Platinum iridium eight-array electrode of the type used in human patients. (**b**) Platinum iridium electrode with a ball at the end of the type used in animal studies The differentiated Schwann cell–like cells were grown in layers on the electrodes in sodium alginate hydrogels for two weeks; healthy Schwann cell–like cells are visible in five to six layers on both cochlear implants (a,b). (**c**) Higher-magnification phase-contrast image of the hydrogel layers on a ball implant. (**d**) Fluorescence micrograph of the same cochlear implant pictured in C. Live/Dead staining was used to distinguish living from dead cells. Ethidium homodimer was used to stain dead cells (orange), and calcein AM was used to stain live cells (green). The implant was coated with hydrogel-encapsulated Schwann cells, which were maintained for two weeks in the encapsulated form and then checked for viability. The scale bar in D, the fluorescence image, applies to both C and D.

could be coated with neurotrophin-expressing Schwann cells that would attract SGN.

Two different types of platinum iridium electrodes (kindly provided by Dr. Bryan Pfingst, Dept. Otolaryngology Head and Neck Surgery, University of Michigan) were "coated" with Schwann cell–like cells or undifferentiated mESC using 1% sodium alginate hydrogel as a scaffold; both types of coated CIs were grown in culture for two weeks (Fig. 6). The cultures were supplemented with fresh media every week. Control electrodes were either uncoated, coated in hydrogel layers without cell inclusions, or coated with undifferentiated mESC in the hydrogel layers. Figure. 6A is a photograph of a CI of the type used in human patients, coated with Schwann cell–like cells in the hydrogel layers (five layers are readily discerned in this photograph). Figure 6B–D are photographs of the type of CI electrode used in animal studies. All are photographs of the same electrode. Five layers of hydrogel containing Schwann cell–like cells are seen in Figure 5B. Figure 5C is a close-up phase-contrast photograph of the electrode ball head. The encapsulated cells were stained for live and dead cells with ethidium bromide and calcein (Live/Dead Cell Viability Assays, Invitrogen, Carlsbad, CA). Large numbers of healthy cells (green) and very few dead cells (orange) were found in the hydrogel layers coated with the Schwann cell–like cells (Fig. 6C) or undifferentiated ESCs (control; not shown) at six weeks in culture.

Extension of Primary Mouse Statoacoustic Ganglion or Spiral Ganglion Neurites Toward the Schwann Cell–like Cell-coated Cochlear Implant, but Not a Bare Cochlear Implant was Seen by Time-lapse Digital Microscopy

CI electrodes of the ball type seen in Figure. 5B–D were then co-cultured with intact primary embryonic mouse statoacoustic ganglia or intact postnatal spiral ganglia, or with neurons dissociated from these ganglia to determine whether the neurites would demonstrate directional outgrowth toward the cell-coated CIs. We monitored the entire interaction by time-lapse digital videography on a specially designed microscope with a gas-supplied (5% CO_2) tissue culture incubator on the stage over five to 14 days.

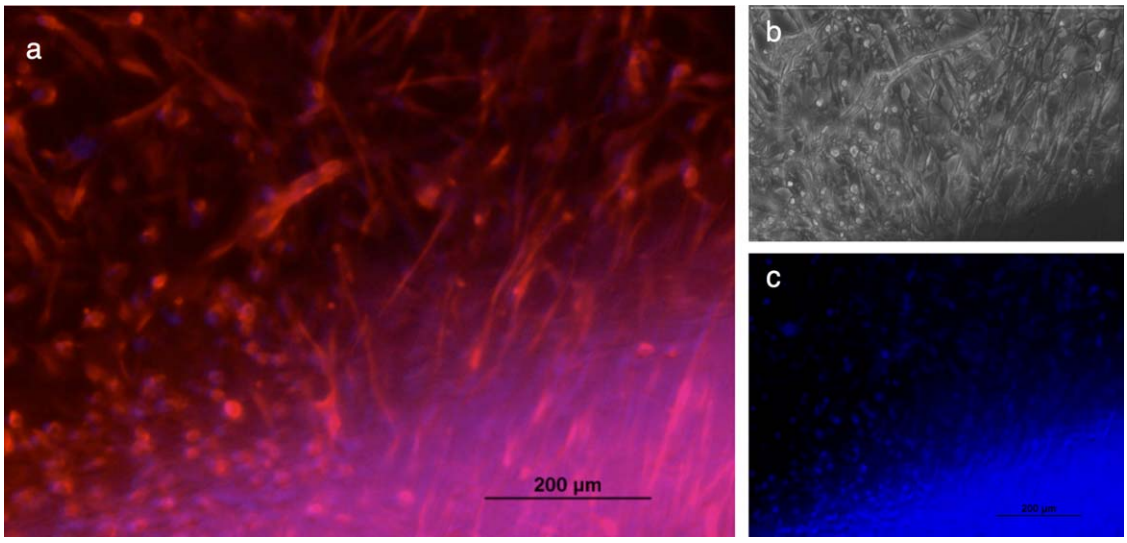

Fig. 7. Neurites of embryonic mouse (E2.5) statoacoustic ganglion interact with Schwann cell–like cells in the hydrogel layers on a ball-type CI at two weeks in culture. At the beginning of the experiment, the statoacoustic ganglion was placed 1 cm away from the Schwann cell–like cell-coated CI on a porcine gel–coated tissue culture dish. Interactions with the cell coats on the implants were followed by time-lapse digital cinematography over the entire two-week period. The processes and some neuronal cell bodies reached the CI after four to five days. These photographs were taken at 13 days. (**a**) Neurites (and some cell bodies) were labeled by immunocytochemistry for Neurofilament 150kDa (Nfil) protein marker and a secondary antibody (Alexa Fluor 580) (red) labels the extensive processes that had reached the CI. The blue crescent of labeling at the bottom represents the DAPI-labeled Schwann cell–like cell nuclei. (**b**) The phase contrast micrograph view of these processes/cells from the statoacoustic ganglion and the implant (same field as A). (**c**) DAPI-stained nuclei of the Schwann cell–like cells are seen in blue within the hydrogel "coats" in this micrograph of the "blue" channel. No directional statoacoustic ganglion neurite outgrowth was seen when the statoacoustic ganglion explants were co-cultured with a bare CI or with a CI coated with hydrogel layers containing undifferentiated stem cells.

Neurite migration and directional outgrowth trajectories were also photographed every 24 hr after addition of the CIs to cultures of the primary ganglia.

We first tested whether primary statoacoustic ganglion neurons exhibited directed neurite outgrowth toward CIs coated with hydrogels that contained Schwann cell–like cells. A co-cultured SAG explant and the Schwann cell–coated CI or a SAG explant and a bare implant were placed 1 cm apart in the tissue culture dish, and a video camera was programmed to capture images at different locations over the dish at 20-min intervals over five to 14 days. We then analyzed the images to observe any evidence of neurite extension or directional outgrowth from the ganglion toward the implant. No directed outgrowth was seen toward bare CIs under any conditions. By contrast, after two days, 87% ± 4% of the processes took the direction toward the Schwann cell–like cell-coated CI, even if during the first two days some outgrowth was random and non-directional. We also observed that the explant itself in some cases split in half and some of the neurons themselves (with and without underlying glial cells) migrated in the CI's direction.

The long-term co-culture (2 weeks) of Schwann cell–like cell-coated CI and statoacoustic ganglia showed directional outgrowth of neurites and extensive contact of neuronal processes on the Schwann cell–like cell-coated CI from both statoacoustic ganglion neuron explants and dissociated cells. No neurite outgrowth whatever was seen toward "bare" CIs, those coated with hydrogel but not cells or implants coated with hydrogels containing undifferentiated mESC. Although some processes were seen emerging from the ganglia under the three "control" conditions (bare implant, hydrogel- but not cell-coated implant, or undifferentiated mESC in the hydrogels), the neurite processes were short, emerged randomly from all sides of the explants, and showed no directionality or appreciable extension even after two weeks.

In marked contrast, from day 3 onward, neuronal processes emerging from the statoacoustic ganglia were observed to turn in the direction of the Schwann cell–like cell-coated CIs and to migrate toward them. The emerging neurites and some migrating cell bodies could be positively stained for Neurofilament marker protein throughout the experiment.

By two weeks, the statoacoustic ganglion neurites had reached the CI (Fig. 7) and had penetrated the hydrogel layers containing Schwann cell–like cells in the hydrogel layers. Figure 7A,B are fluorescence micrograph (Fig. 7A) and phase-contrast micrograph (Fig. 7B) of the same part of the coated electrode surface. In Figure, 7A, Neurofilament 150kDa (Nfil) (red) was used to label the neuronal processes and a few cell bodies. In this double-labeled photograph, the blue staining (DAPI) is associated with the Schwann cell–like cell nuclei. These are more clearly visible in Figure 7A, where the DAPI-stained nuclei are heavily concentrated close to the electrode head and seen to belong to the Schwann cell–like cells (compare Fig. 7C with 7A). A few neuronal cell bodies that stained with DAPI are seen in the area above the concentrated Schwann cell layers (Fig. 7C).

Directional Outgrowth of Neurites from SGN was Seen Toward a Variety of Targets

Spiral ganglia isolated from the six-day-old postnatal mouse cochlea were also co-cultured with bare CIs or with hydrogel-coated CIs containing Schwann cell–like cells or undifferentiated mESC. We used the same culturing techniques, cinematographic and photographic techniques, to observe neurite extension and

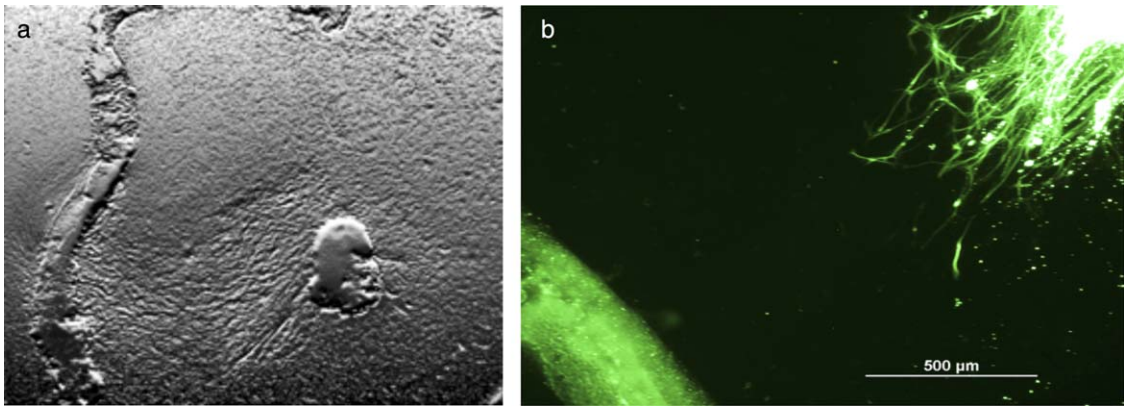

Fig. 8. Interaction of primary spiral ganglion neurites (mouse postnatal day 3) (**a**) and processes from MIF-induced neuron-like cell neurites (**b**) with wild-type organ of Corti explants in culture. (a) Polarized image of a primary mouse spiral ganglion (right) extending extensive neurites directionally toward a wild-type organ of Corti explant (at left). No directional outgrowth was seen toward a MIF-knockout mouse organ of Corti (not shown). This was also demonstrated in separate experiments detailed in Bank et al., 2012, (Fig. 6 in that work). (b) MIF-induced neuron-like cells stained with acetylated tubulin (green) cultured with a wild-type organ of Corti explant for a week showed fasciculated neurites (approaching form the right) growing toward the wild-type organ of Corti (at lower left) No such outgrowth was seen toward OC explants from MIF-knockout mice (as was also demonstrated for primary spiral ganglion neuronal processes in Bank et al., 2012, Fig. 6).

document any directional outgrowth both under the light microscope and by time-lapse live-cell imaging. At the experiment's end, the cultures were stained for Neurofilament and DAPI. Again, we found that directional neurite outgrowth was seen only toward the Schwann cell–like cell-coated CIs. Initially, as with the primary statoacoustic ganglia, at least some outgrowth of neurites was observed 360° around the cluster of spiral ganglion neuronal cell bodies. After the third day of co-culture, the majority (91±6%) of the neurites showed directional outgrowth toward the Schwann cell–like cell-coated CI, and processes reached the implant by eight to nine days in culture. Neurite outgrowth from SGNs in the presence of a bare CI or one coated with undifferentiated mES cells showed little extension and no directional outgrowth at all, even after two weeks in co-culture (data not shown).

These migration and directional outgrowth studies demonstrate that a Schwann cell–like cell-encapsulated CI could potentially deliver directional molecular cues to attract neurites of an endogenous adult spiral ganglion. Importantly, we had previously demonstrated that receptors for MIF remain on SGNs into adulthood (Bank et al., 2012).

Neuron-like mESC-derived Cells' Directional Outgrowth Toward Targets

The MIF-induced/DHA-enhanced neuron-like cells were assessed after a week of co-culture for directional migration and directional outgrowth toward organ of Corti explants derived from six-day-old postnatal mouse cochleae (wild-type or derived from a MIF knockout mouse) as described in our previous studies (Bank et al., 2012); a bare CI; c) a CI coated with Schwann cell–like cells; a CI coated with undifferentiated mESC; a hydrogel-coated CI without cells. The neuron-like cells exhibited few emerging processes and no directional neurite outgrowth toward the bare CI, the hydrogel-coated (no encapsulated cells) CI, or the mESC-coated CI. In contrast neuron-like cells co-cultured with the Schwann cell–like cell-CI showed long processes, rapid migration, and directional outgrowth toward the CI (71±11% of the processes were oriented toward the CI). However, these processes became so fasciculated that measurements of total "oriented" processes became difficult over time.

MIF-induced neuron-like cells co-cultured with the six-day-old postnatal wild-type mouse organ of Corti explants showed clusters of neurites with growth cones and multiple branches growing toward the wild-type organ of Corti (Fig. 8B). Compare this outgrowth with the robust neurite outgrowth emerging from a wild-type primary SGN toward the wild-type organ of Corti explant seen in Figure 8A. Little outgrowth, random emergence of processes, and no directional outgrowth of neurites was seen if the organ of Corti explant came from an MIF knockout mouse. These data recapitulate our finding with primary neurons and organ of Corti explants. Neither statoacoustic ganglion neurites nor spiral ganglion neurites emerged toward an MIF knockout organ of Corti explant (Bank et al., 2012). These studies indicate that the MIF-/DHA-induced neuron-like cells derived after three weeks of exposure to the neurotrophic cytokine MIF and DHA can migrate toward appropriate targets in vitro. Functionality is being tested electrophysiologically. However, directional outgrowth and electrophysiological function remain to be thoroughly tested when such electrodes are implanted in vivo in animal models.

Discussion

Concomitant Differentiation of Neuron-like Cells and Schwann cell–like Cells in a Microfluidic Device

Two novel stem cell–based therapeutic strategies for producing cell populations that could be used to alleviate sensorineural hearing loss have been assessed in these studies. We have differentiated a common population of mESCs (Doetschman et al., 1985; Roth et al., 2007; Roth et al., 2008, Bank et al., 2012) into neuron-like and Schwann cell–like cells simultaneously in a slow-flow microfluidic device.

These studies were based on earlier work in which we used conventional tissue culture for such differentiation studies. Our lab had produced the first embryonic stem cell–based model of both the myelinating and non-myelinating Schwann cell in 2007

(Roth et al., 2007; Roth et al., 2008). We also induced mESCs to take on neuronal phenotypes with different characteristics depending on which neurotrophin was used as the inducing agent (NGF or CNTF) (Roth et al., 2007; Roth et al., 2008; MIF: Bank et al., 2012). In these studies, we also used Neuregulin (as in Roth et al., 2007; Roth et al., 2008) to induce the mESC to become Schwann cell–like on the "Schwann cell" side of the microfluidic device.

Although both NGF and CNTF served as the "control" neuron-inducing agents in the microfluidic studies, we used MIF as the inducing neurotrophic cytokine in most of the studies detailed here both in the microfluidic model and in additional tissue culture–based experiments. This was because we had previously demonstrated that MIF is the first neurotrophin expressed in the developing inner ear (Holmes et al, 2011; Shen et al., 2012; Bank et al., 2012) that it is responsible for the earliest steps in both neurogenesis and directional neurite outgrowth, and that it is a neuronal survival factor (Bank et al., 2012). We had also previously demonstrated that inner ear SGNs retain the appropriate receptors for MIF into adulthood (Bank et al., 2012). The neuron-like cells induced by MIF in either conventional tissue culture dishes (Bank et al. 2012) or, as we show here, microfluidic devices, can bear significant resemblance to inner ear SGNs (Bank et al., 2012). The use of DHA enhances the maturation of such "neurons" in conventional tissue culture and in the microfluidic devices.

In the microfluidic devices, concomitant neuronal cell–type specific differentiation was seen and documented in morphological, molecular, and electrophysiological assays in the devices themselves. These devices spare both cells and reagents and are labor-saving because the reservoirs supply a continuously delivered source of medium and factors (Fig. 1C,D, cartoons). Neuron-like cells extended processes over the Schwann cell lawns (Fig. 1A), and interactions between the "neurons" and "Schwann cells" resulted in the early steps of myelination (Fig. 4). We had previously demonstrated such directional outgrowth and early steps in myelination in conventional tissue culture experiments (Roth et al., 2008). The proximity of the two differentiating cell populations in the device is as critical for development of mature properties in both populations as it is in vivo. Without intimate contact with neurons, Schwann cells do not develop myelin components, nor, of course, do they myelinate any cells in their environment except neurons. The role of MIF in myelination is under study in a number of systems. Disrupting pathways known to be downstream of MIF, such as Jab1, are known to cause dysmyelination (Porrello et al., 2011). Such pathways can be easily studied in these microfluidic devices and in model organisms such as the Zebrafish (Weber et al., in preparation), as in more comprehensive studies of the events in myelination (Han et al., 2013; Glenn and Talbot, 2013).

The extremely slow flow maintained in the microfluidic device over three weeks allows for the accumulation of autocrine and paracrine factors that would ordinarily be washed through the device if the flow rate were accelerated (Park et al., 2009). This slow flow also allows for interactions between the two differentiating cell populations that emerge from the common population of ES cells—neuron-like and Schwann cell–like cells. The two cell populations differentiate "side by side," and interactions between them can be documented.

We addressed the role of MIF in the observed directional outgrowth of neuron-like cells to the "Schwann cell" side of the device by inhibiting MIF's downstream effects in one of two ways: use of the biochemical MIF inhibitor 4-IPP, as we had done previously (Shen et al., 2012), or use of a function-blocking antibody to MIF, again as we had done in previous studies (Bank et al., 2012). We found that blocking MIF by either of these means on the Schwann cell side of the device once the embryonic stem cells had differentiated into Schwann cell–like cells, we could significantly reduce *directional* neurite outgrowth over the Schwann cell lawn, no matter which neurotrophin was used to induce the neuron-like phenotype (Fig. 2). However, the greatest effect was seen if MIF was the inducing agent or if MIF were enhanced with DHA. Note that blocking MIF did not totally eliminate directed neurite outgrowth over the Schwann cell lawn. This is because Schwann cells are known to produce another neurotrophic cytokine, monocyte chemoattractant protein 1 (MCP1), which also is produced by sensory hair cells of the inner ear (Bank et al., 2012), and which we have shown to affect both directional neurite outgrowth from inner ear neurons and their survival (Bianchi et al., 2005; Bank et al., 2012). The effect of blocking MCP1 was not tested in these experiments.

Meeting a Long-term Objective: Producing a Stem Cell–derived Neuronal Population That Phenotypically Has Some Resemblance to That of the Inner Ear's SGN

One objective of these studies is to produce a stem cell–derived population of neuron-like cells that could potentially replace lost or damaged SGNs in human patients, potentially using a patient's own induced pluripotent stem cells (Oshima et al., 2010) as a source of such neurons that could alleviate sensorineural hearing loss.

Researchers have previously attempted to develop glutamatergic neurons from ES cells by transient expression of neurogenin 1 and supplementation with BDNF and GDNF. These neurons were found to have some characteristics of SGNs, including electrophysiological functionality (Reyes et al., 2008). The "neurons" were also implanted in an animal model (Reyes et al., 2008), although no functional improvement of a malfunctioning auditory system was demonstrated.

More promising later studies from the Rivolta Group demonstrated that some significant improvement in hearing function could be achieved in a deafened gerbil model (Chen et al., 2012) when human embryonic inner ear stem cells were implanted into the deafened animals. However, the derivation of neurons from human inner ear stem cells required a complex multi-step, multi-week in vitro protocol for neuronal differentiation before implanting the cells. By contrast to these complex differentiation protocols, the ES-to-neuron conversion described here and in our previous studies requires only a single step with recombinant MIF (Bank et al. 2012). It is worth emphasizing that MIF is the inner ear's earliest expressed neurotrophin, and that this neurotrophic cytokine controls gangliogenesis in the vertebrate inner ear (Shen et al., 2012; Bank et al., 2012). Its use in eliciting a neuronal population is preferable to the use of NGF, CNTF or cytokines, largely because we have also demonstrated that adult SGN retain receptors for MIF (Bank et al., 2012).

Therapeutic Potential: a Neuronal Replacement Strategy

Neuron-like cells derived from MIF- and DHA-induced ES cells could potentially be used in the future to replace lost or damaged

sensory neurons of the SG in adults. However, if this paradigm is to be successful, several important hurdles will have to be met, some of which would be incurred in optimizing the neuronal cell implant procedure itself, and some of which involve meeting critical criteria for monitoring functional connections of the "neuronal" population to the organ of Corti if the implant were to be successful.

First, the cells must have cellular, molecular, and electrophysiological properties sufficiently similar to the cells they replace to be functionally "competent" in situ. Second, any implanted substitute "neuronal" population would have to remain viable and capable of extending "neurites" in vivo, toward a source of molecular cues that could provide directional signals and sustain their survival.

MIF is exactly such a neuronal directional outgrowth and survival factor (Holmes et al., 2011; Shen et al., 2012; Bank et al., 2012). MIF is produced in the native organ of Corti by the supporting cells that underlie each sensory hair cell and by the Schwann cells of the inner ear (Bank et al., 2012). The neurite outgrowth documented in these microfluidic studies demonstrates that the neuron-like cells also respond to chemoattractant-producing (MIF-producing) Schwann cells in the microfluidic devices. Either a function-blocking antibody to MIF (Bank et al., 2012) or the biochemical MIF 4-IPP (Shen et al., 2012) can prevent directed outgrowth of these neuron-like cells toward the Schwann cell target cells, demonstrating that MIF production by the Schwann cell–like cells is a key feature of the neuron-like cells' directed outgrowth. A MIF-producing Schwann cell–like cell-coated CI could also provide such cues and is discussed later in this section.

The number of surviving "neuron-like" cells has to be sufficient to provide functionally viable "neurons" over the number of days required for their neuronal processes to reach the target tissue (surviving hair cells in the organ of Corti, presumably via the MIF-producing supporting cells that cup each sensory hair cell) or the CI.

If the target tissue is the native organ of Corti, the implant site would have to be optimized and two additional critical criteria would have to be met: The implanted cells cannot form a tumor or dedifferentiate and proliferate, even if the cell bolus that eventually forms is benign.

In the future, in order to prevent tumor formation in the inner ear, once the spiral ganglion neuronal processes have contacted the CI, a cell suicide cassette could be triggered to eliminate the Schwann cell–like cells (Li et al., 2012), the cell debris of which would presumably be removed by macrophages. Slow-release gels (Inaoka et al., 2009) that release recombinant MIF could also be used to coat the CIs, but even with slow release, the supply of MIF in these gels would eventually be exhausted. It is not known how long it would be necessary to supply MIF to ensure that a maximum number of spiral ganglion neuronal processes reach the implant and form functional contacts. Using a stem cell–based source of MIF could provide the cytokine for a much longer time. The possibility of infection must also be minimized.

How far have we come toward realizing these criteria? MIF and DHA are capable of inducing some properties in the mESC-derived neurons that are similar to those of SGNs under the conditions of the experiment, including VgluT1 (a marker for SGNs of the inner ear) transporter expression and protein, which was documented in MIF- and DHA-induced neuron-like cells.

However, the transporter is also expressed to the same extent in NGF- or CNTF-induced mESC-derived neurons, each of which could also provide a viable source of "neurons." Also, there is electrophysiological excitability and the possibility of action potentials: Ion channel expression was assessed by RTqPCR and at the protein level by immunocytochemistry. The neuron-like cells' physiological properties were evaluated by whole-cell patch clamping. We were encouraged by the preliminary electrophysiological experiments showing that MIF+DHA could induce a neuronal population with promising electrophysiological properties. No inward or outward currents were found when electrophysiological recordings were made from the neuron-like cells induced by either NGF or NGF+DHA.

The cells also expressed ion channels (sodium and potassium channels) that are expected for SGNs (Greenwood et al., 2007; Xie et al., 2007), but sodium channel protein expression was better defined in the immunohistochemistry labeling experiments than potassium ion channel expression on the neurites.

These experiments demonstrate that these neuron-like cells express *some* functionally mature properties in common with SGNs under in vitro conditions. We have not yet documented action potentials under any of these conditions; such recordings will be attempted in the future.

Functionally mature neuron-like mESC-derived cells were experimentally tested for directional neurite outgrowth when co-cultured with a CI or primary explanted organ of Corti target under in vitro conditions. They exhibited directional outgrowth toward both the Schwann cell–like cell-coated CI and wild-type, but not the MIF knockout mouse organ of Corti explants in culture. Therefore, neuron-like cells derived from mESC using MIF and DHA could potentially be implanted as a stem cell–based therapy in patients with low SG counts who are not presently candidates for CI therapy.

Potential of ESC-derived Schwann Cell–like Cells for Alleviating Sensorineural Hearing Loss

The second embryonic stem cell–based therapeutic approach described in these studies is the production of mESC-derived Schwann cell–like cells. These cells are potentially capable of *continuous production* of molecular cues, including MIF and MCP1, that could improve the number of connections between any remaining SGNs and a Schwann cell–like cell-coated cochlear implant.

In these studies, Schwann cell–like cell-coated cochlear implants in vitro were studied for their ability to "attract" neurites from both *primary* embryonic statoacoustic ganglion and the mature spiral ganglion. Eventually, such a strategy might be employed to enhance the functionality of a CI. If successful, this could lead to improved hearing or better speech perception in patients experiencing hearing loss.

Schwann cells are known to be important for peripheral nerve regeneration (Bhatheja and Field, 2006; Gambarotta et al., 2013). These properties depend on their state of differentiation (e.g., quiescent, proliferating, or mature Schwann cells) (Baehr and Bunge, 1989; Kidd et al, 2013; Salzar, 2012; Salzar 2015; Grigoryan and Birchmeier, 2015).

In earlier studies by other investigators, the effects of factors secreted by Schwann cells were examined on a quasi-neuronal model composed of PC12 cells, which are, in some investigators' estimations, a model for neuronal cells, which were tested for cell

survival and "neurite" outgrowth (Bampton and Taylor, 2005). In these experiments, Schwann cell–conditioned medium was tested on "neurite" outgrowth from PC12 cells against a range of isolated factors known to be secreted by Schwann cells. This conditioned medium showed clear neuritogenic effects and suggested that Schwann cells are likely candidates for promoting neuronal regeneration (Bampton and Taylor, 2005; see also Wissel et al., 2008).

Other groups have reported enhanced survival of SGNs in animal models of hearing loss by implanting Schwann cells, which were molecularly engineered to provide sustained delivery of neurotrophins such as BDNF (Bunge, 1993; Girard et al., 2005; Golden et al., 2007; Pettingill et al., 2008). Such an engineered population of Schwann cells was used to coat a CI, with some success in attracting SGNs to the implant (Pettingill et al., 2008).

However, the group attributed the attraction of the SGNs to the Schwann cells on the implant to the engineered neurotrophin expression and release by the Schwann cells. While this could indeed be the reason, it is also possible that since all Schwann cell express MIF, MIF was either the main source of or contributed to the attraction.

If this cell-coated CI strategy were to be successful, initially after cochlear implant was introduced, electrical impedance should be higher due to the presence of the hydrogel-encapsulated cells, but the biocompatible and biodegradable hydrogel might release the cells in the perilymph or area surrounding the CI, which could potentially provide sustained neurotrophin release, which would also serve to protect the SGNs. Once the hydrogel has completely degraded after releasing all the cells, the CI's own electrical stimulation would presumably function normally, but this has not been examined either in vitro or in a living animal.

Combining Stem Cell–based Strategies

Various combinations of these approaches could be used. Neuron-like (especially potentially spiral ganglion–like) embryonic stem cell–derived cells could be implanted into an inner ear in which hair cell degeneration has begun but not yet progressed to complete loss. Potential stem cell sources could include a human patient's own induced pluripotent stem cells (iPSC) (Oshima et al., 2010). Alternatively, stem cell–derived Schwann cell–like cells that are capable of sustained delivery of critical supporting factors like MIF could be used to coat a CI. Recall that all Schwann cells, including these engineered Schwann cell–like cells, produce MIF (Huang et al., 2002a,b; Bank et al., 2012). The research studies outlined here are limited to in vitro conditions; in the future, this approach can be applied in animal models in in vivo studies.

Conclusions

These studies provide first steps toward producing MIF-induced stem cell–derived neurons that could resemble SGNs sufficiently to replace lost or damaged SGNs. Furthermore, Neuregulin-induced Schwann cell–like cells that produce MIF could be used to "coat" a CI that provides a source of MIF to which both immature and mature auditory system neurons respond. We had earlier demonstrated that both neuronal subtypes retain MIF receptors (Bank et al., 2012). Thus, a common population of "stem cells," which in this report are mESCs but in the future could be host-derived iPSCs, can be induced to form two populations of cells that could provide viable approaches for auditory system repair.

Experimental Procedures

Culturing mES Cells

Cell lines: The cell line used for these studies was the D3 mES cell line (ATCC-CRL-1934; Doetschman et al., 1985). 10,000 mESC D3 cells were plated onto 0.1% porcine gel–coated (Sigma) 48 well Primaria plates (Falcon), and cells were differentiated over a three-week period, using our previously reported methods (Roth et al., 2007; Roth et al., 2008). Undifferentiated mES cells (controls) were fed basal medium daily, while cells in neuronal differentiation media and Schwann cell differentiation medium were fed every third day. Media Preparation: Proliferating/undifferentiated (ES medium): 81% DMEM (Invitrogen) without phenol red, but including 1% L-Glut, 1% Pen/Strep, 1% nonessential amino acids (Invitrogen), 15% FBS (Atlanta Biological, Lawrenceville, GA), 1% sodium pyruvate (2% stock, Sigma Aldrich, St. Louis, MO), 7 μL/L mercaptoethanol (Sigma Aldrich), 1,000 U/mL ESGRO (Chemicon, Temecula, CA).

Differentiation of mES Cell into Schwann Cell–like Cells in Vitro

Our previously published methods were used to produce Schwann cell differentiation (Roth et al., 2007; Roth et al., 2008). The medium consisted of 500 mL alpha-modified MEM (GIBCO 41061-029), 6% day-11 chick embryo extract (prepared in-house), 10% heat-inactivated FBS, 58 μL Gentamicin (Invitrogen), 10 μL Neuregulin1 (NRG1) (R&D Systems).

Differentiation of mES Cell into Various Neuron-like Cell Types in Vitro

Neuronal differentiation: 95% F-12 (Invitrogen), 1% Pen/Strep (Invitrogen), 1% N2 (Invitrogen), 2% B27 (Invitrogen), 2% sodium pyruvate (2% stock), 0.5 μg/L bFGF (R&D Systems, Minneapolis, MN), 1 μg/L IL-7, 5 μg/L IGF-1 (Sigma), or for specific neuronal cell types: 1 μg/L CNTF (R&D Systems) for motor neuron-like neurons (Roth et al., 2007); 1 μg/L nerve growth factor (NGF; Millipore, Billerica MA) (sensory neuron-like cells; Roth et al., 2007); MIF 1 μg/mL (R&D Systems), + 5 μM DHA (Nu Chek Prep Inc., Elysian, MN). DHA-supplemented media included: CNTF and 5 μM DHA, NGF and 5 μM DHA, MIF and 5 μM DHA (Bank et al., 2012). To block MIF release from Schwann cell–like cells, either the biochemical MIF inhibitor 4-IPP (Specs, Delft, Netherlands) at 0.1 μM (Shen et al., 2012) or the MIF function-blocking monoclonal antibody under our previously described conditions (Bank et al., 2012) were added to the Schwann cell reservoir. These MIF-blocking strategies were used *only* on the Schwann cell side of the device once the cells had differentiated.

Assessing Directed Differentiation of D3 Cells into Neuron-like Cells

After three weeks of growth, cells were labeled for expression of Neurofilament marker (NF150) (neuronal differentiation marker). Antibodies (Chemicon, MA) were diluted in 5% normal goat serum (Chemicon) in 0.1% tween 20/phosphate buffered saline

(PBS) (Sigma). Cells were fixed in 4% paraformaldehyde (Sigma) and treated with primary antibody NF150 (R&D systems) at 1:500 dilution followed by secondary antibody Alexa Fluor 590 at 1:200 dilution (Invitrogen, CA) and DAPI (1:1000 dilution) stain for the cell nucleus. Photomicrographs were taken with a light microscope or using appropriate filters on a Leica inverted fluorescence microscope. We repeated each set of experimental conditions at least three times in separate experiments. The differentiated cells were labeled by our previously reported ICC techniques (Roth et al., 2007) for ion channel protein expression with antibodies (Abcam, Cambridge, MA) to sodium channel (SP19) and potassium channel (Kv3.1).

Isolation and Culture of Primary Mouse Statoacoustic Ganglia Neuron (Statoacoustic Ganglion)

Statoacoustic ganglia from Balb/C mouse embryos (E15.5–E17.5) were isolated from the two ears as previously described (Germiller et al., 2004; Bank et al., 2012) and rinsed in PBS (Bianchi and Raz, 2004; Bank et al. 2012). The whole ganglia were then plated on 0.1% porcine gel–treated Primaria plates or 0.1% porcine gel–coated glass cover slips (Roth et al., 2008) with the addition of 0.5 mL F12 neuronal basal media (Invitrogen) and incubated overnight for attachment at 37 °C in a cell culture incubator with 5% CO_2. Under some conditions, the statoacoustic ganglia were dissociated and plated as individual neurons as previously described (Bianchi et al., 2005; Bank et al., 2012).

Electrophysiological Recordings of mESC-derived Neuron-like Cells; Patch Clamp Whole-cell Recording

Whole-cell current- and voltage-clamp recordings were performed on cells selected for a bipolar neuron-like morphology with long processes. These recordings were made at room temperature using an Axopatch 200B amplifier with a Digidata 1200 or 1322A digitizer (Molecular Devices, Sunnyvale, CA). Data were acquired using pCLAMP 9 software (Molecular Devices). Glass electrodes were pulled from borosilicate capillaries (World Precision Instruments, Sarasota, FL) to achieve an electrical resistance of 3–6 M. Electrodes were filled with an internal solution containing (in mM): 112 KCl, 2 MgCl2, 0.1 CaCl2, 11 EGTA, 10 HEPES, 5 Na2 + ATP, and buffered to pH 7.2 with KOH. The external solution contained (in mM): 137 NaCl, 5 KCl, 1.7 CaCl2, 1 MgCl2, 10 HEPES, 16 glucose and buffered to pH 7.2 with NaOH.

Isolation of Organ of Corti and Explant Culture

A modification of the method of Parker et al., (Parker et al., 2010) was used to isolate mouse Organ of Corti as previously described (Bank et al., 2012). Day 6 neonatal Balb/C mice were first decapitated and the outer skin was removed using a scalpel blade. The skull and the brain were bisected to expose the temporal bone, and the tissue and the bones surrounding the temporal bone were removed. The temporal bone was rinsed in sterile PBS and transferred to a new plastic 50-mm dish, and the cochlea was removed under a surgical microscope. The bony labyrinth was carefully separated and the apex of the organ of Corti was exposed to visualize the basal cochlea after the removal of the labyrinth. Using fine forceps, the base was held and the OC carefully removed and unwound. The isolated OC explants were positioned on 1% porcine gel–coated Primaria (Falcon) plates with 0.5 mL F12 basal media and incubated at 5%CO_2 in a tissue culture incubator overnight.

Isolation of Primary Spiral Ganglia and Spiral Ganglion Neurons

Once the OC explant was isolated, the modiolus of the cochlea was cut in half and the tissue was minced using a scalpel blade. SGN tissue explants were placed on 0.1% porcine gel–coated Primaria tissue culture plates with 0.5 mL F12 media and incubated overnight in order to promote attachment as previously described (Bank et al., 2012).

Simultaneous Differentiation of Neuron-like Cells and Schwann Cell–like Cells in a Microfluidic Device

Device preparation and maintenance: The microfluidic device itself and all tubes, pipette tips (used as reservoirs), and equipment were sterilized by the same autoclaving and UV sterilizing procedures used in previous studies (Park et al., 2009). Polydimethylsiloxane (PDMS) microfluidic chambers were autoclaved and subsequently were oxygen plasma–treated so that the channel was hydrophilic. Assembly and operation of the microfluidic system was done in a tissue culture hood under positive pressure to prevent possible contamination. To prevent air bubble formation initially, a PBS solution–filled 1000-μL pipette tip was inserted into the outlet port, and by the force of gravity PBS was allowed to flow slowly into the main channel without producing any air bubbles in the channel. Air bubble formation at all stages of loading, cell seeding, and growth was carefully examined microscopically. None of the many devices used in these experiments developed air bubbles/locks either initially or during the course of the experiment or the ensuing analysis.

The microfluidic devices were designed according to previous specifications (Fig. 1) (Park et al., 2009). Microfluidic chambers and tubing were made hydrophilic and sterilized by oxygen plasma and UV treatment, respectively. Devices were prefilled with PBS by inserting a 1000-μL pipette tip into the outlet and allowing PBS to fill the chamber by gravity-driven flow. Air bubbles were avoided by maintaining liquid (PBS, culture medium) on top of the device, thereby preventing bubble formation due to evaporation or due to connection of pipette tips. Devices were coated with 0.1% porcine gel for 2 hr under UV light before cell seeding. mESchwann < zaq;30>cells were trypsinized and seeded into devices at a density of 10,000 cells/mL and allowed to adhere overnight at 37 °C and 5% CO_2. When the mESC were fully attached, an osmotic pump was connected to tubing at the outlet channel and 1-mL pipette tip reservoirs containing either neuronal differentiation or Schwann cell differentiation media were inserted into the appropriate inlets (Park et al., 2009). Devices, including osmotic pumps and inlet and PEG reservoirs, were incubated at 37 °C and 5% CO_2 over three weeks, with the PEG and inlet reservoirs replaced once every seven days.

Assessment of Cell Type Differentiation and Myelination in a Microfluidic Device

At various time points during the three-week period, cells were fixed with 4% PFA and labeled with either antibody to Neurofilament heavy chain protein (200kDa), a general marker for neurons; VgluT1, a putative marker for mature "auditory system–

like" neurons; or MBP, a marker for Schwann cell myelination (Bodhireddy et al., 1994; Roth et al., 2007, Roth et al., 2008; Salzer, 2012; Salzer 2015). Fluorescent images were taken of five sections of the microfluidic device to observe the overall pattern of neurite outgrowth from the neuron-like cells derived from the mESC and neurite extension over the mESC-derived Schwann cell–like cell lawns in the other side of the device, as well as any evidence of myelination.

COMSOL Simulation

A COMSOL simulation was performed to correlate simulated concentration profiles of soluble factors to the observed growth patterns in the device. Microfluidic device geometry was imported into COMSOL Multiphysics 4.2 (COMSOL, Inc.). Fluid density and viscosity were set based on previous measurements, and laminar flow average velocities were set at the two inlets (1.4 μm/sec) and outlet (2.8 μm/sec) based on volumetric flow measurements as described in Medium Viscosity Measurement. To ensure a fully developed profile, entrance and exit lengths were set to 1000 times greater than 0.06*Re*D, where *Re* and D are Reynolds number of flow and tubing diameter, respectively. A laminar flow solver was used to generate flow profiles, which, due to the extremely slow flow, allowed diffusive mixing of growth factors and cytokines at the interface of the two separate laminar streams. Concentration profiles of relevant soluble factors were analyzed by the dilute species transport model. Diffusion coefficients were selected to match previous results for molecules with similar molecular weights: 1.5×10^{-10}, 4.25×10^{-10}, and 1.27×10^{-10} m^2/sec for MIF (Durand et al., 2009), DHA (Culbertson et al., 2002), and NGF (Lawrence et al., 2009) (or CNTF, since molecular weights are similar), respectively. A quad mesh system with minimum element size of 3.1×10^{-7} and maximum element size of 0.154 mm was generated to fully capture flow and concentration profiles within the channel for steady laminar flow.

Neurite Measurement

Either the MetaMorph Neurite Outgrowth Measurement program or NIH ImageJ software (downloaded from the internet: https://imagej.nih.gov/ij/) was used to measure total neurite outgrowth and length of "neurites" under a variety of conditions (Figs. 1, 2). Briefly, thresholds were adjusted so that intensity levels for fluorescent detection were 50% above the background grayscale (MetaMorph instruction manual) (Universal Imaging, documented: T20029). Settings were then optimized for cell body size before calculating the above parameters.

Even though neurites extended only micrometers in the microfluidic device, photographs were taken at magnification of 20X in the Leica inverted microscope. Using MetaMorph or ImageJ software, we were able to analyze the photomicrographs at the maximum pixel size, representing the neurite measurement in microns in length. The mean outgrowth could not be normalized to cell numbers because neurite outgrowth extends from clusters of the mES cells that are individually indistinguishable.

Statistical Analysis

For quantification of the MetaMorph and ImageJ data, all the experiments were run at the minimum in triplicate (e.g., n = 8 for all conditions analyzed in Fig. 2). Differences between treatment groups were analyzed using Mann-Whitney U-tests performed in MATLAB. Single-tailed tests were performed using the rank-sum function, and significance levels were computed exactly using the "method" "exact" option.

Coating a Cochlear Implant with Hydrogel-encapsulated Schwann Cell–like Cells

The Schwann cell–like cells were differentiated from mESC following our previously published procedures (Roth et al., 2007) and trypsinized using 0.5% trypsin-EDTA. The cells were counted and diluted to 10,000 cells/mL and centrifuged at 1000 rpm for 5 min. The cell pellet was re-suspended in 1 mL of Schwann cell differentiation media and 1 mL 2% sodium alginate (hydrogel) tissue culture grade (Pronovo SLG100, Novomatrix) to bring the hydrogel concentration to 1%. To optimize cell growth in alginate gels, we had first tested different concentrations of sodium alginate, 0.5–2.0%, which was used for encapsulating the SCs at 10,000 cells/mL. We also tested gel polymerization achieved with different concentrations of calcium chloride (50 mM–300 mM). Optimized conditions for "Schwann cell" viability and gel firmness were determined to be 1% sodium alginate and 200 mM calcium chloride for gel polymerization.

The cells were thoroughly mixed with alginate and placed in an ice bath. The CI was coated with hydrogel in order to support Schwann cell growth by a modification of the method of Winter et al. (Winter et al., 2007), and each implant was monitored daily under a light microscope to determine if Schwann cell growth was limited to the vicinity of the electrode. The electrode was initially dipped in an ice-cold 200 mM $CaCl^2$ solution, followed by dipping in the hydrogel-cell mixture solution. This step was repeated to cover hydrogel-cell mixture on the CI up to 2–3 mm up to 5–6 layers of coating. Then the whole hydrogel-cell and CI setup was placed in an ice-cold 200-mM $CaCl^2$ solution for 10 min. Once polymerization was complete, the electrode was placed on a tissue culture plate (35 mm Falcon) and the encapsulated SC allowed to grow for two days with Schwann cell medium supplementation (Roth et al., 2007). After we observed that the Schwann cell encapsulation was successful, the Schwann cell population was tested for survivability. The encapsulated cells were checked for viability using the Live/Dead stain (Invitrogen following the manufacturer's protocol. The cells were stained for ethidium homodimer (orange indicates dead cells) and calcein (green for the live cells). The Schwann cell–coated CI was then used for co-culture studies with primary statoacoustic ganglion or SGNs, or with mESC-derived "neurons" induced by the various inducing agents/cytokine.

Co-cultures of Neuron-like Cells with OC Explants, Bare Cochlear Implant, or "Schwann Cell"-coated Cochlear Implants

Neuron-like cells were differentiated from mES cells with MIF on porcine gel–coated glass coverslips for two to three weeks; mouse organ of Corti explants (prepared as described) were placed in the same 35-mm Falcon Primaria TC plate at a distance of 1 cm to study directional neurite outgrowth toward the target (OC). The cells were cultured and fed with F12 basal media for five days, and neurite outgrowth was observed both by time-lapse digital micrography and, at end stage, by ICC staining for TUJ1 for neuron-specific class III beta-tubulin. Interactions between the

neuron-like cells and the "Schwann cell"-coated CI were monitored in "real time" by placing the mESC-derived Schwann cell–like cell-coated CI or bare CI with the differentiated neuron-like cells for five days. Directional outgrowth was observed and photomicrographs were taken in time-lapse mode at various locations in the culture dish every 20 minutes. ICC at "end stage" was performed by fixing the preparation in 4% PFA followed by Neurofilament marker as primary mouse antibody, followed by TUJ1 primary antibody, followed by Alexa Fluor 488-conjugated anti-mouse secondary antibody (Invitrogen). Photomicrographs were taken using a Leica inverted fluorescence microscope.

Co-culture of MIF-induced Neuron-like Cells or Spiral Ganglia with Bare Cochlear Implant, ES Cochlear Implant, and Schwann Cell–coated Cochlear Implant

SG (mouse P3) explants were cultured alone for two days to promote strong attachment to the 0.1% porcine gel–coated plate, and then a bare CI or the "Schwann cell"-encapsulated CI was placed 1 cm away from the SG explant. Neurite outgrowth and neurite contact with the "Schwann cell" CI or bare CI were monitored for five days, and photomicrographs were taken at 24-hr intervals using a light microscope. Schwann cell (CI) and SGN interactions and neurite outgrowth were also monitored in live time-lapse imaging for two to four days post positioning of the ganglion explant using a live-cell imaging station DeltaVision microscope in the Microscopy and Image Analysis Laboratory of the Cell and Developmental Biology Department. The camera was assigned (by computer) to visit different locations repeatedly around the plate. The camera was programmed to revolve around the explant and capture time-lapse images at 20-min intervals. The actual setup of the experiment is shown in Figure 6.

RTqPCR Assessment of Putative SGN Marker Expression

The expression of a variety of SGN-"specific" markers was performed by RTqPCR using our previously published methods (Germiller et al., 2004; Bank et al., 2012 and modification of methods in Chen et al., 2011), using the primer pairs specified in those publications.

Total RNA was extracted from whole statoacoustic ganglion, whole spiral ganglia, and mESC-derived neuronal cultures (+DHA as described above) at roughly three-day intervals over a 30-day period; or from co-cultures of mESC-derived "neurons" grown on mESC-derived SC lawns (as in Roth et al., 2008). Total RNA was extracted using an RNeasy mini kit (Qiagen), reverse-transcribed with Superscript II RNase H minus reverse transcriptase (Invitrogen), and amplified using SYBR Green-based PCR (Applied Biosystems). Controls included DNase I treatment during RNA isolation and reverse transcriptase-minus and non-template controls during PCR. The sequences of the PCR products were confirmed in the University of Michigan's DNA Sequencing Core.

Acknowledgments

This work was supported by grants from the NIH (NIH/NIDCD 2RO1DC04184-04, 3R01DC004184-08W12, and R01 DC006436-04A2) to K.F.B.; NSF (IOS 0930096) to K.F.B.; Deafness Research Foundation (DRF) to K.F.B.; NIHT32 DE007057 to P.R.; NIH 5T32EB005582-05 (Microfluidics in Biotechnology) to P.R., NSF DGE 0718128 to J.B.W. (ID: 2010101926) and R25 GM086262 to F.M. The authors would like to thank Dr. Robin Davis, Department of Neuroscience, Rutgers University, for extensive discussions and advice on the design of primer pairs for identification of SGN-specific markers, as well as providing primer pairs for some of the ion channels analyzed in her studies; Dr. Steven H. Green of the University of Iowa for extensive discussions on the development of SGNs and their stage-specific characteristics; Dr. Ethan M. Jewett, UC Berkeley Departments of Statistics and Computer Science, for the statistical study design and computations, for redesign of some of the figures, and for editing the article; members of the Barald and Takayama labs for comments on the article and suggestions for additional experimental approaches using microfluidics.

References

Altschuler RA, O'Shea KS, Miller JM. 2008. Stem cell transplantation for auditory nerve replacement. Hear Res 242:110–116.

Altschuler RA, Cho Y, Ylikoski J, Pirvola U, Magal E, Miller JM. 1999. Rescue and regrowth of sensory nerves following deafferentation by neurotrophic factors. Ann N Y Acad Sci 884:305–311.

Baehr M, Bunge RP. 1989. Functional status influences the ability of Schwann cells to support adult rat retinal ganglion cell survival and axonal regrowth. Exp Neurol 106:27–40.

Bampton ET, Taylor JS. 2005. Effects of Schwann cell secreted factors on PC12 cell neuritogenesis and survival. J Neurobiol 63: 29–48.

Bank LM, Bianchi LM, Ebisu F, Lerman-Sinkoff D, Smiley EC, Shen Y, Ramamurthy P, Thompson DL, Roth TM, Beck CR, Flynn MJ, Teller RS, Feng L, Llewellyn GN, Holmes BB, Sharples C, Coutinho-Budd J, Linn SA, Chervenak AP, Dolan DF, Benson J, Kanicki A, Martin C, Altschuler R, Jewett EM, Koch A, Germiller JA, Barald, KF. 2012. Macrophage Migration Inhibitory Factor (MIF) acts as a neurotrophin for neurons in the developing mammalian and avian inner ears. Development 139:4666–4674 (cited in Faculty of 1000).

Barald KF, Kelley MW. 2004. From placode to polarization: new tunes in inner ear development. Development 131:4119–4130.

Bermingham-McDonogh O, Rubel EW. 2003. Hair cell regeneration: winging our way toward a sound future. Curr Opin Neurobiol 13: 119–126.

Bianchi LM, Daruwalla Z, Roth TM, Attia NP, Lukacs NW, Richards AL, White IO, Allen SJ, Barald KF. 2005. Immortalized mouse inner ear cell lines demonstrate a role for chemokines in promoting the growth of developing statoacoustic ganglion neurons. J Assoc Res Otolaryngol 6:355–367.

Bianchi LM, Raz Y. 2004. Methods for providing therapeutic agents to treat damaged spiral ganglion neurons. Curr Drug Targets CNS Neurol Disord 3:195–199.

Bhatheja K, Field J. 2006. Schwann cells: origins and role in axonal maintenance and regeneration. Int J Biochem Cell Biol 38:1995–1999.

Bodhireddy SR, Lyman WD, Rashbaum WK, Weidenheim KM. 1994. Immunohistochemical detection of myelin basic protein is a sensitive marker of myelination in second trimester human fetal spinal cord. J Neuropathol Exp Neurol 53:144–149.

Bodmer D. 2008. Protection, regeneration and replacement of hair cells in the cochlea: implications for the future treatment of sensorineural hearing loss. Swiss Med Wkly 138:708–712.

Boomkamp SD, Riehle MO, Wood J, Olson MF, Barnett sc. 2012. The development of a rat in vitro model of spinal cord injury demonstrating the additive effects of Rho and ROCK inhibitors on neurite outgrowth and myelination. Glia 60:441–56.

Breuskin I, Bodson M, Thelen N, Thiry M, Nguyen L, Belachew S, Lefebvre PP, Malgrange B. 2008. Strategies to regenerate hair cells: identification of progenitors and critical genes. Hear Res 236:1–10.

Bunge R, Moya F, Bunge M. 1981. Observations on the role of Schwann cell secretion in Schwann cell—axon interactions. Adv Biochem Psychopharmacol 28:229–242.

Bunge RP. 1991. Schwann cells in central regeneration. Ann N Y Acad Sci 633:229–233.
Bunge RP. 1993. Expanding roles for the Schwann cell: ensheathment, myelination, trophism and regeneration. Curr Opin Neurobiol 3:805–809.
Bunge RP. 1994. The role of the Schwann cell in trophic support and regeneration. J Neurol 242:S19–21.
Burns JC, Corwin JT. 2013. A historical to present-day account of efforts to answer the question: "what puts the brakes on mammalian hair cell regeneration?". Hear Res 297:52–67.
Callizot N, Combes M, Steinschneider R, Poindron P. 2011. A new long term in vitro model of myelination. Exp Cell Res 317:2374–2383.
Cao D, Kevala K, Kim J, Moon HS, Jun SB, Lovinger D, Kim HY. 2009. Docosahexaenoic acid promotes hippocampal neuronal development and synaptic function. J Neurochem 111:510–521.
Chen W, Jongkamonwiwat N, Abbas L, Eshtan SJ, Johnson SL, Kuhn S, Milo M, Thurlow JK, Andrews PW, Marcotti W, Moore HD, Rivolta MN. 2012. Restoration of auditory evoked responses by human ES-cell-derived otic progenitors. Nature 490:278–282
Chen WC, Xue HZ, Hsu YL, Liu Q, Patel S, Davis RL. 2011. Complex distribution patterns of voltage-gated calcium channel α-subunits in the spiral ganglion. Hear Res 278:52–68.
Chen WC, Davis RL. 2006. Voltage-gated and two-pore-domain potassium channels in murine spiral ganglion neurons. Hear Res 222:89–99.
Chen WC, Xue HZ, Hsu YL, Liu Q, Patel S, Davis RL. 2007. Subunits of voltage-gated calcium channels in murine spiral ganglion cells. Acta Otolaryngol, 127:8–12.
Coleman B, Fallon JB, Pettingill LN, de Silva MG, Shepherd RK. 2007. Auditory hair cell explant co-cultures promote the differentiation of stem cells into bipolar neurons. Exp Cell Res 313:232–243.
Corrales CE, Pan L, Li H, Liberman MC, Heller S, Edge AS. 2006. Engraftment and differentiation of embryonic stem cell-derived neural progenitor cells in the cochlear nerve trunk: growth of processes into the organ of Corti. J Neurobiol 66:1489–1500.
Culbertson CT, Jacobson SC, Ramsey JM. 2002. Diffusion coefficient measurements in microfluidic devices. Talanta 56:365–373.
Davis RL, Liu Q. 2011. Complex primary afferents: What the distribution of electrophysiologically-relevant phenotypes within the spiral ganglion tells us about peripheral neural coding. Hear Res 276:34–43.
de Felipe MM, Feijoo Redondo AF, Garcia-Sancho J, Schimmang T, Alonso MB. 2011. Cell- and gene-therapy approaches to inner ear repair. Histol Histopathol 26:923–940.
Defourny J, Lallemend F, Malgrange B. 2011. Structure and development of cochlear afferent innervation in mammals. Am J Physiol Cell Physiol 301:C750–761.
Doetschman TC, Eistetter H, Katz M, Schmidt W, Kemler R. 1985. The in vitro development of blastocyst-derived embryonic stem cell lines: Formation of visceral yolk sac, blood islands and myocardium. J Emb Exp Morph 87:27–45.
Duran Alonso MB, Feijoo-Redondo A, Conde de Felipe M, Carnicero E, Garcia AS, Garcia-Sancho J, Rivolta MN, Giraldez F, Schimmang T. 2012. Generation of inner ear sensory cells from bone marrow-derived human mesenchymal stem cells. Regen Med 7:769–783.
Durand NF, Saveriades E, Renaud P. 2009. Detecting proteins complex formation using steady-state diffusion in a nanochannel. Anal Bioanal Chem 394:421–425.
Evans AJ, Thompson BC, Wallace GG, Millard R, O'Leary SJ, Clark GM, Shepherd RK, Richardson RT. 2009. Promoting neurite outgrowth from spiral ganglion neuron explants using polypyrrole/BDNF-coated electrodes. J Biomed Mater Res A 91:241–250.
Flores-Otero J, Xue HZ, Davis RL. 2007. Reciprocal regulation of presynaptic and postsynaptic proteins in bipolar spiral ganglion neurons by neurotrophins. J Neurosci 27:14023–14034.
Gambarotta G, Fregnan F, Gnavi S, Perroteau I. 2013. Neuregulin 1 role in Schwann cell regulation and potential applications to promote peripheral nerve regeneration. Int Rev Neurobiol 108:223–256.
Géléoc GS, Holt JR. 2014. Sound strategies for hearing restoration. Science 344:1241062.
Germiller JA, Smiley EC, Ellis AD, Hoff JS, Deshmukh I, Allen SJ, Barald KF. 2004. Molecular characterization of conditionally immortalized cell lines derived from mouse early embryonic inner ear. Dev Dyn 231:815–827.
Gingras M, Beaulieu MM, Gagnon V, Durham HD, Berthod F. 2008. In vitro study of axonal migration and myelination of motor neurons in a three-dimensional tissue-engineered model. Glia 56:354–364.
Girard C, Bemelmans AP, Dufour N, Mallet J, Bachelin C, Nait-Oumesmar B, Baron-Van Evercooren A, Lachapelle F. 2005. Grafts of brain-derived neurotrophic factor and neurotrophin 3-transduced primate Schwann cells lead to functional recovery of the demyelinated mouse spinal cord. J Neurosci 25:7924–7933.
Glenn TD, Talbot WS. 2013. Signals regulating myelination in peripheral nerves and the Schwann cell response to injury. Curr Opin Neurobiol 23:1041–1048.
Golden KL, Pearse DD, Blits B, Garg MS, Oudega M, Wood PM, Bunge MB. 2007. Transduced Schwann cells promote axon growth and myelination after spinal cord injury. Exp Neurol 207:203–217.
Goodman I, Golden G, Flitman S, Xie K, McConville M, Levy S, Zimmerman E, Lebedeva Z, Richter R, Minagar A, Averback P. 2007. A multi-center blinded prospective study of urine neural thread protein measurements in patients with suspected Alzheimer's disease. J Am Med Dir Assoc 8:21–30.
Greenwood D, Jagger DJ, Huang LC, Hoya N, Thorne PR, Wildman SS, King BF, Pak K, Ryan AF, Housley GD. 2007. P2X receptor signaling inhibits BDNF-mediated spiral ganglion neuron development in the neonatal rat cochlea. Development 134:1407–1417.
Grigoryan T, Birchmeier W. 2015. Molecular signaling mechanisms of axon-glia communication in the peripheral nervous system. Bioessays 37:502–513.
Han H, Myllykoski M, Ruskamo S, Wang C, Kursula P. 2013. Myelin-specific proteins: A structurally diverse group of membrane-interacting molecules. Biofactors. 39:233–241.
Heinen A, Kremer D, Hartung HP, Kury P. 2008. p57 kip2's role beyond Schwann cell cycle control. Cell Cycle 7:2781–2786.
Holmes KE, Wyatt MJ, Shen YC, Thompson DA, Barald KF. 2011. Direct delivery of MIF morpholinos into the zebrafish otocyst by injection and electroporation affects inner ear development. J Vis Exp pii:2466.
Hsu SH, Ni HC. 2009. Fabrication of the microgrooved/microporous polylactide substrates as peripheral nerve conduits and in vivo evaluation. Tissue Eng Part A 15:1381–1390.
Houle JD, Ye JH. 1999. Survival of chronically-injured neurons can be prolonged by treatment with neurotrophic factors. Neuroscience 94:929–936.
Hu Z, Ulfendahl M, Olivius NP. 2004a. Central migration of neuronal tissue and embryonic stem cells following transplantation along the adult auditory nerve. Brain Res 1026:68–73.
Hu Z, Ulfendahl M, Olivius NP. 2004b. Survival of neuronal tissue following xenograft implantation into the adult rat inner ear. Exp Neurol 185:7–14.
Hu Z, Ulfendahl M, Olivius NP. 2005. NGF stimulates extensive neurite outgrowth from implanted dorsal root ganglion neurons following transplantation into the adult rat inner ear. Neurobiol Dis 18:184–192.
Huang T, Qin J, Xiong S, Yu L, Huo X, Liao H, Li J, Liu D. 2002a. [Expression of macrophage migration inhibitory factor mRNA in Schwann cells]. Zhonghua Wai Ke Za Zhi [Chinese Journal of Surgery] 40:699–701.
Huang T, Qin JQ, Huo XK, Yu L, Xiong SH, Liu DY, Zhong SZ. 2002b. [Changes in content of macrophage migration inhibitory factor secreted by Schwann cells after peripheral nerve injury] Zhonghua wai ke za zhi [Chinese Journal of Surgery] 40:702–707.
Hurley PA, Crook JM, Shepherd RK. 2007. Schwann cells revert to non-myelinating phenotypes in the deafened rat cochlea. Eur J Neurosci 26:1813–1821.
Inaoka T, Nakagawa T, Kikkawa YS, Tabata Y, Ono K, Yoshida M, Tsubouchi H, Ido A, Ito J. 2009. Local application of hepatocyte

growth factor using gelatin hydrogels attenuates noise-induced hearing loss in guinea pigs. Acta Otolaryngol 129:453–457.
Ito J, Endo T, Nakagawa T, Kita T, Kim TS, Iguchi F. 2005. A new method for drug application to the inner ear. ORL J Otorhinolaryngol Relat Spec 67:272–275.
Ito K, Yoshiura Y, Ototake M, Nakanishi T. 2008. Macrophage migration inhibitory factor (MIF) is essential for development of zebrafish, Danio rerio. Dev Comp Immunol 32:664–672.
Jarjour AA, Zhang H, Bauer N, Ffrench-Constant C, Williams A. 2012. In vitro modeling of central nervous system myelination and remyelination. Glia 60:1–12.
Jhaveri SJ, Hynd MR, Dowell-Mesfin N, Turner JN, Shain W, Ober CK. 2009. Release of nerve growth factor from HEMA hydrogel-coated substrates and its effect on the differentiation of neural cells. Biomacromolecules 10:174–183.
Jiang H, Sha SH, Forge A, Schacht J. 2006. Caspase-independent pathways of hair cell death induced by kanamycin in vivo. Cell Death Differ 13:20–30.
Jun SB, Hynd MR, Dowell-Mesfin NM, Al-Kofahi Y, Roysam B, Shain W, Kim SJ. 2008. Modulation of cultured neural networks using neurotrophin release from hydrogel-coated microelectrode arrays. J Neural Eng 5:203–213.
Khedr EM, Farghaly WM, Amry Sel-D, Osman AA. 2004. Neural maturation of breastfed and formula-fed infants. Acta Paediatr 93:734–738.
Kidd GJ, Ohno N, Trapp BD. 2013. Biology of Schwann cells. Handb Clin Neurol 115:55–79.
Kondo T, Johnson SA, Yoder MC, Romand R, Hashino E. 2005. Sonic hedgehog and retinoic acid synergistically promote sensory fate specification from bone marrow-derived pluripotent stem cells. Proc Natl Acad Sci U S A 102:4789–4794.
Kyritsis N, Kizil C, Zocher S, Kroehne V, Kaslin J, Freudenreich D, Iltzsche A, Brand M. 2012. Acute inflammation initiates the regenerative response in the adult zebrafish brain. Science 38: 1353–1356.
Landry TG, Wise AK, Fallon JB, Shepherd RK. 2011. Spiral ganglion neuron survival and function in the deafened cochlea following chronic neurotrophic treatment. Hear Res 282:303–313.
Lawrence BJ, Devarapalli M, Madihally SV. 2009. Flow dynamics in bioreactors containing tissue engineering scaffolds. Biotechnol Bioeng 102:935–47.
Liazoghli D, Roth AD, Thostrup P, Colman DR. 2012. Substrate Micropatterning as a New in Vitro Cell Culture System to Study Myelination. ACS Chem Neurosci 3:90–95.
Li H, Liu H, Heller S. 2003. Pluripotent stem cells from the adult mouse inner ear. Nature Med 9:1293–1299.
Li H, Roblin G, Liu H, Heller S. 2003. Generation of hair cells by stepwise differentiation of embryonic stem cells. Proc Natl Acad Sci U S A 100:13495–13500.
Li J, Zhang G, Liu T, Gu H, Yan L, Chen B. 2012. Construction of a novel vector expressing the fusion suicide gene yCDglyTK and hTERT-shRNA and its antitumor effects. Exp Ther Med 4:442–448.
Liu Q, Chen P, Wang J. 2014. Molecular mechanisms and potentials for differentiating inner ear stem cells into sensory hair cells. Dev Biol 390:93–101.
Mellado Lagarde MM, Wan G, Zhang L, Gigliello AR, McInnis JJ, Zhang Y, Bergles D, Zuo J, Corfas G. 2014. Spontaneous regeneration of cochlear supporting cells after neonatal ablation ensures hearing in the adult mouse. Proc Natl Acad Sci U S A 111:16919–16924.
Mena MA, Garcia de Yebenes J. 2008. Glial cells as players in parkinsonism: the “good,” the “bad,” and the “mysterious” glia. Neuroscientist 14:544–60.
Merkus P, Di Lella F, Di Trapani G, Pasanisi E, Beltrame MA, Zanetti D, Negri M, Sanna M. 2014. Indications and contraindications of auditory brainstem implants: systematic review and illustrative cases. Eur Arch Otorhinolaryngol 271:3–13.
Miller JM, Miller AL, Yamagata T, Bredberg G, Altschuler RA. 2002. Protection and regrowth of the auditory nerve after deafness: neurotrophins, antioxidants and depolarization are effective in vivo. Audiol Neurootol 7:175–179.
Monzack EL, Cunningham LL. 2013. Lead roles for supporting actors: critical functions of inner ear supporting cells. Hear Res 303:20–29.
Namgung U. 2015. The Role of Schwann Cell-Axon Interaction in Peripheral Nerve Regeneration. Cells Tissues Organs. 200:6–12.
Nayagam BA, Muniak MA, Ryugo DK. 2011. The spiral ganglion: connecting the peripheral and central auditory systems. Hear Res 278:2–20.
Nave KA, Werner HB. 2014. Myelination of the nervous system: mechanisms and functions. Ann Rev Cell Dev Biol 30:503–533.
Nishio Y, Nishihira J, Ishibashi T, Kato H, Minami A. 2002. Role of macrophage migration inhibitory factor (MIF) in peripheral nerve regeneration: anti-MIF antibody induces delay of nerve regeneration and the apoptosis of Schwann cells. Mol Med. 2002 8:509–520.
O’Leary SJ, Richardson RR, McDermott HJ. 2009. Principles of design and biological approaches for improving the selectivity of cochlear implant electrodes. J Neural Eng 6:055002.
Oshima K, Shin K, Diensthuber M, Peng AW, Ricci AJ, Heller S. 2010. Mechanosensitive hair cell-like cells from embryonic and induced pluripotent stem cells. Cell 141:704–716.
Paino CL, Fernandez-Valle C, Bates ML, Bunge MB. 1994. Regrowth of axons in lesioned adult rat spinal cord: promotion by implants of cultured Schwann cells. J Neurocytol 23:433–452.
Paivalainen S, Nissinen M, Honkanen H, Lahti O, Kangas SM, Peltonen J, Peltonen S, Heape AM. 2008. Myelination in mouse dorsal root ganglion/Schwann cell cocultures. Moll Cell Neurosci 37:568–578.
Pan GJ, Chang ZY, Schöler HR, Pei D. 2002. Stem cell pluripotency and transcription factor Oct4. Cell Res 12:321–329.
Park JY, Kim SK, Woo DH, Lee EJ, Kim JH, Lee SH. 2009. Differentiation of neural progenitor cells in a microfluidic chip-generated cytokine gradient. Stem Cells 27:2646–2654.
Parker M, Brugeaud A, Edge AS. 2010. Primary culture and plasmid electroporation of the murine organ of Corti. J Vis Exp pii: 1685.
Parkins CW. 1985. The bionic ear: principles and current status of cochlear prostheses. Neurosurgery 16:853–865.
Pettingill LN, Minter RL, Shepherd RK. 2008. Schwann cells genetically modified to express neurotrophins promote spiral ganglion neuron survival in vitro. Neuroscience 152:821–828.
Pettingill LN, Richardson RT, Wise AK, O’Leary SJ, Shepherd RK. 2007. Neurotrophic factors and neural prostheses: potential clinical applications based upon findings in the auditory system. IEEE Trans Biomed Eng 54:1138–1148.
Pettingill LN, Wise AK, Geaney MS, Shepherd RK. 2011. Enhanced auditory neuron survival following cell-based BDNF treatment in the deaf guinea pig. PLoS One 6:e18733.
Pfingst BE, Zhou N, Colesa DJ, Watts MM, Strahl SB, Garadat SN, Schvartz-Leyzac KC, Budenz CL, Raphael Y, Zwolan TA. 2015. Importance of cochlear health for implant function. Hear Res 322:77–88.
Phan PA, Tadros SF, Kim Y, Birnbaumer L, Housley GD. 2010. Developmental regulation of TRPC3 ion channel expression in the mouse cochlea. Histochem Cell Biol 133:437–448.
Porrello E, Dina G, Panattoni M, Triolo D, Cerri F, Del Carro U, Comi F, Wrabetz L, Feltri ML, Pardi R, Quattrini A, Previtali SC. 2011. CSN5/Jab1 inactivation in Schwann cells causes dysmyelinating peripheral neuropathy. J Peripher Nerv Syst 16:S111–112.
Ramekers D, Versnel H, Grolman W, Klis SF. 2012. Neurotrophins and their role in the cochlea. Hear Res 288:19–33.
Reyes JH, O’Shea KS, Wys NL, Velkey JM, Prieskorn DM, Wesolowski K, Miller JM, Altschuler RA. 2008. Glutamatergic neuronal differentiation of mouse embryonic stem cells after transient expression of neurogenin 1 and treatment with BDNF and GDNF: in vitro and in vivo studies. J Neurosci. 28:12622–12631.
Roehm PC, Hansen MR. 2005. Strategies to preserve or regenerate spiral ganglion neurons. Curr Opin Otolaryngol Head Neck Surg 13:294–300.
Roehm PC, Xu N, Woodson EA, Green SH, Hansen MR. 2008. Membrane depolarization inhibits spiral ganglion neurite growth via activation of multiple types of voltage sensitive calcium channels and calpain. Mol Cell Neurosci 37:376–387.
Roth TM, Ramamurthy P, Muir D, Wallace MR, Zhu Y, Chang L, Barald KF. 2008. Influence of hormones and hormone metabolites on the growth of Schwann cells derived from embryonic

stem cells and on tumor cell lines expressing variable levels of neurofibromin. Dev Dyn 23:513–524.
Roth TM, Ramamurthy P, Ebisu F, Lisak RP, Bealmear BM, Barald KF. 2007. A mouse embryonic stem cell model of Schwann cell differentiation for studies of the role of neurofibromatosis type 1 in Schwann cell development and tumor formation. Glia 55: 1123–1133.
Salzer JL. 2012. Axonal regulation of Schwann cell ensheathment and myelination. J Peripher Nerv Syst 17:14–9.
Salzer JL. Schwann cell myelination. 2015. Cold Spring Harb Perspect Biol 7:a020529.
Sato T, Doi K, Taniguchi M, Yamashita T, Kubo T, Tohyama M. 2006. Progressive hearing loss in mice carrying a mutation in the p75 gene. Brain Res 1091:224–234.
Shen Y, Thompson DL, Kuah MK, Wong KL, Wu KL, Linn SA, Jewett EM, Shu-Chien AC, Barald KF. 2012. The cytokine macrophage migration inhibitory factor (MIF) acts as a neurotrophin in the developing inner ear of the zebrafish, Danio rerio. Dev Biol 363:84–94.
Shi F, Edge ASB. 2013. Prospects for replacement of auditory neurons by stem cells. Hear Res 297:106–112.
Shibata SB, Budenz CL, Bowling SA, Pfingst BE, Raphael Y. 2011. Nerve maintenance and regeneration in the damaged cochlea. Hear Res 281:56–64.
Taupin P. 2011. Neurogenic drugs and compounds to treat CNS diseases and disorders. Cent Nerv Syst Agents Med Chem 11: 35–37.
Torisawa YS, Chueh BH, Huh D, Ramamurthy P, Roth TM, Barald KF, Takayama S. 2007. Efficient formation of uniform-sized embryoid bodies using a compartmentalized microchannel device. Lab Chip 7:770–776.
Uauy R, Hoffman DR, Peirano P, Birch DG, Birch EE. 2001. Essential fatty acids in visual and brain development. Lipids 36:885–895.
Wan G, Corfas G, Stone JS. 2013. Inner ear supporting cells: rethinking the silent majority. Semin Cell Dev Biol 24:448–459.
Wei Y, Gong K, Zheng Z, Liu L, Wang A, Zhang L, Ao Q, Gong Y, Zhang X. 2010. Schwan-like cell differentiation of rat adipose-derived stem cells by indirect co-culture with Schwann cells in vitro. Cell Prolif 43:606–616.
Winter JO, Cogan SF, Rizzo JF 3rd. 2007. Neurotrophin-eluting hydrogel coatings for neural stimulating electrodes. J Biomed Mater Res B Appl Biomater 81:551–563.
Winter JO, Gokhale M, Jensen RJ, Cogan SF, Rizzo JF. 2008. Tissue Engineering Applied to the Retinal Prosthesis: Neurotrophin-Eluting Polymeric Hydrogel Coatings. Mater Sci Eng C Mater Biol Appl 28:448–453.
Wise AK, Fallon JB, Neil AJ, Pettingill LN, Geaney MS, Skinner SJ, Shepherd RK. 2011. Combining cell-based therapies and neural prostheses to promote neural survival. Neurotherapeutics 8:774–787.
Wise AK, Hume CR, Flynn BO, Jeelall YS, Suhr CL, Sgro BE, O'Leary SJ, Shepherd RK, Richardson RT. 2010. Effects of localized neurotrophin gene expression on spiral ganglion neuron resprouting in the deafened cochlea. Mol Ther 18:1111–1122.
Wissel K, Stover T, Hofmann NS, Chernajovsky Y, Daly G, Sasse S, Warnecke A, Lenarz T, Gross G, Hoffmann A. 2008. Fibroblast-mediated delivery of GDNF induces neuronal-like outgrowth in PC12 cells. Otol Neurotol 29:475–481.
Xie D, Hu P, Xiao Z, Wu W, Chen Y, Xia K. 2007. Subunits of voltage-gated calcium channels in murine spiral ganglion cells. Acta Otolaryngol 127:8–12.
Yang IH, Gary D, Malone M, Dria S, Houdayer T, Belegu V, McDonald JW, Hakor N. 2012. Axon myelination and electrical stimulation in a microfluidic, compartmentalized cell culture platform. Neuromolecular Med 14:112–118.
Yang L, Su J, Zhang X, Jiang C. 2008. Hypercapnia modulates synaptic interaction of cultured brainstem neurons. Respir Physiol Nerobiol 160:147–159.
Yang T, Kersigo J, Jahan I, Pan N, Fritzsch B. 2011. The molecular basis of making spiral ganglion neurons and connecting them to hair cells of the organ of Corti. Hear Res 278:21–33.
Zhang H, Yang R, Wang Z, Lin G, Lue TF, Lin CS. 2011. Adipose tissue-derived stem cells secrete CXCL5 cytokine with neurotrophic effects on cavernous nerve regeneration. J Sex Med 8:437–446.
Zhang X, Zeng Y, Zhang W, Wang J, Wu J, Li J. 2007. Co-transplantation of neural stem cells and NT-3-overexpressing Schwann cells in transected spinal cord. J of Neurotrauma 24: 1863–1877.
Zhang YQ, Zeng X, He LM, Ding Y, Li Y, Zeng YS. 2010. NT-3 gene modified Schwann cells promote TrkC gene modified mesenchymal stem cells to differentiate into neuron-like cells in vitro. Anat Sci Int 85:61–67.
Zhong SX, Liu ZH. 2004. Immunohistochemical localization of the epithelial sodium channel in the rat inner ear. Hear Res 193:1–8.